Research Square

Preprints are preliminary reports that have not undergone peer review.
They should not be considered conclusive, used to inform clinical practice,
or referenced by the media as validated information.

Identification of PLEKHA4 in the antiviral network by pairwise analysis of critical hubs and its regulation by Interferons, TLR ligands, and Respiratory Viruses

Ramana Chilakamarti

ramana181@gmail.com

University of Massachusetts Lowell https://orcid.org/0000-0002-5153-8252

Research Article

Keywords: Bioinformatics, Protein-Protein Interaction (PPI) Network, Interferon-Stimulated Genes (ISGs), STAT1, PLEKHA4, Acute Lung Injury, Respiratory Viruses

Posted Date: November 23rd, 2026

DOI: https://doi.org/10.21203/rs.3.rs-11808162/v1

License: This work is licensed under a Creative Commons Attribution 4.0 International License.
Read Full License

Additional Declarations: The authors declare no competing interests.

Research Square

Identification of PLEKHA4 in the antiviral network by pairwise analysis of critical hubs and its regulation by Interferons, TLR ligands, and Respiratory Viruses

Chilakamarti V. Ramana [*]
ORCID ID: 0000-0002-5153-8252

[*]Correspondence should be addressed:
Chilakamarti V. Ramana, Ph.D.
E-mail: ramana181@gmail.com

Abstract

Type I interferon (IFN) regulates intricate transcriptional networks, critical for antiviral defense, cell growth, and immunomodulation. Identifying novel hubs in these networks will provide new insights into innate immune regulation and highlight potential therapeutic targets for viral diseases. Using a pairwise common protein interaction partner analysis method (PIC-VENN), we identified novel hubs within the core type I IFN-driven signaling network, focusing on STAT1, STAT2, and PML. We investigated candidate hubs across multiple functional genomics datasets. Network analysis identified a novel hub, PLEKHA4, within the IFN-driven antiviral network, which plays a major role in developmental pathways and cancer. Analysis of several protein interaction databases revealed that PLEKHA4 interacted with multiple key network hubs, including STAT1, STAT2, STAT3, PML, and SMARCA4. PLEKHA4 was rapidly and sustainably induced in both human and murine cell types following stimulation with type I and type II interferons. We found that IFN-α-mediated PLEKHA4 expression depended on STAT1, but not IRF7. PLEKHA4 expression was significantly upregulated *in vitro* and *in vivo* following Toll-like receptor (TLR) activation. Transcriptomic data confirmed that PLEKHA4 expression serves as a molecular marker in mouse models of acute lung injury (ALI) and in response to pathogenic respiratory viruses. PLEKHA4 is highly co-expressed with canonical antiviral mediators during acute inflammatory, bacterial, and viral lung diseases, highlighting its key role in innate immunity and its potential as a therapeutic target for severe respiratory diseases.

Keywords: Bioinformatics; Protein-Protein Interaction (PPI) Network; Interferon-Stimulated Genes (ISGs); STAT1; PLEKHA4; Acute Lung Injury; Respiratory Viruses.

1 Introduction

Highly infectious respiratory viruses such as H1N1 influenza and Severe Acute Respiratory Syndrome Coronavirus 2 (SARS-CoV-2) cause seasonal epidemics and pose serious threats to global health, increasing mortality and morbidity (1,2). After infection with a respiratory virus, localized immune sentinel cells in the lungs, such as macrophages, natural killer cells, and dendritic cells, mount a robust antiviral response by producing large quantities of pro-inflammatory cytokines and interferons (3,4). Interferons (IFNs) are a family of pleiotropic cytokines that regulate the expression of hundreds of genes involved in cellular metabolism, apoptosis, immune response, and antiviral responses (5,6). Innate immunity relies heavily on Type I IFN (IFN-α/β), whereas adaptive immunity depends on Type II IFN (IFN-γ), which is mainly secreted by activated $CD8^+$ T cells (7,8). Clinical studies on human genetic variants linked to inborn errors of immunity, along with research using knockout mouse models, have well documented the importance of Type I IFN signaling in viral clearance (9,10). Studies on severe COVID-19 patients have identified both disruptive genetic defects in Type I IFN pathway components and a high rate of neutralizing autoantibodies targeting these critical cytokines (11,12). Conversely, severe COVID-19 tissue samples often show hyper-inflammatory profiles with an imbalanced overexpression of inflammatory and interferon-stimulated genes (ISGs) (13).

Interferon signaling is mediated by activating transcription factors and regulatory proteins that bind to genomic DNA to modulate its structure and regulate gene expression. For Type I IFNs, this transcriptional induction unfolds in two distinct phases. First, IFN-α/β binds to its cognate surface receptor, activating the JAK-STAT cascade. This leads to rapid assembly of STAT1 homodimers and a trimeric regulatory complex known as interferon-stimulated gene factor-3 (ISGF-3), consisting of STAT1, STAT2, and IRF9 (5,6). After tyrosine phosphorylation and nuclear translocation, these transcription factors bind specific promoter motifs known as gamma-activated sequences (GAS) and interferon-stimulated response elements (ISRE) (14).

Beyond this immediate response, Type I IFN signaling induces an additional group of transcription factors at the mRNA level within a few hours to sustain prolonged, multi-phase transcriptional activity. Global studies of these transcription factors highlighted three primary functional subnetworks: antiviral response, immunomodulation, and cell growth regulation (15,16). At the cellular level, post-translational modifications such as phosphorylation drive protein-protein interactions in these signaling cascades, fine-tuning mammalian growth factor and cytokine pathways (17).

The core architecture of the Type I IFN antiviral response, which is conserved through evolution, is tightly regulated by an interactive protein network centered on three major transcription factor families: Signal Transducers and Activators of Transcription (STAT), Interferon Regulatory Factors (IRF), and Speckled Proteins (SP) (15). Because transcription factors with related biological functions often share downstream genomic targets and physical interaction partners, mapping these networks is highly informative. Topological pairwise analyses of essential signaling hubs have uncovered previously obscured nodes and functional modules connecting innate and adaptive immunity (18). We used the Protein Interaction Connectome-VENN (PIC-VENN) methodology to evaluate STAT1 and its main antiviral Type I IFN hub partners. Protein interaction network modeling showed that multiple uncharacterized proteins participate in the antiviral signaling pathway. In addition to known antiviral hubs such as STAT3, MAVS, TRIM25, and BRCA1, our analysis identified novel signaling hubs including ESR2, SMARCA4, FBXW7, and PLEKHA4. Previous studies showed that PLEKHA4 is located in the plasma membrane, interacts with phosphoinositides, and is involved in developmental cell signaling through the Wnt pathway (19,20). The PLEKHA4 gene has been well studied for its role in cancer biology. It is frequently upregulated in various human tumors, where it promotes cell growth, migration, and survival by interacting with key signaling pathways like Wnt/β-catenin and mitogen-activated protein kinase (MAPK) pathways (20). However, its

precise role within interferon networks and broader immunity remains unclear, prompting this investigation. Supporting this work, our screening of diverse transcriptomic datasets confirmed that Type I IFN signaling and TLR ligands regulated PLEKHA4 expression in multiple cell types and after exposure to various respiratory viruses.

2 Materials and Methods

2.1 Protein Interaction Databases

We used protein interaction databases, including the Search Tool for the Retrieval of Interacting Genes/Proteins (STRING), BioGRID, and the Wiki resource on human protein interactions (WIKI-PI) (21–23). We retrieved all entries regarding the protein interaction partners of the signaling hubs from WIKI-PI or BioGRID. We visualized the hubs and nodes within the protein interaction networks using the built-in software tools available in the BioGRID and STRING databases. Regulatory functional relationships between hubs within the signaling network were analyzed using software suites from the Database for Annotation, Visualization and Integrated Discovery (DAVID), Metascape, the Kyoto Encyclopedia of Genes and Genomes (KEGG), and the Transcriptional Regulatory Relationships Unravelled by Sentence-based Text (TRRUST) databases (24–27). We performed Protein Interactions Connectome-Venn (PIC-VENN) analysis of antiviral hubs in type I interferon (IFN) signaling as described previously (18).

2.2 Gene Expression Datasets and Analysis

We used standard bioinformatics tools as previously described (15,18). We retrieved baseline tissue expression data for PLEKHA4 from the Genotype-Tissue Expression (GTEx) database (28, www.gtexportal.org). We obtained single-cell profiles from the Lung Cell Atlas and PLEKHA4 protein

expression profiles across normal and tumor tissues from the Human Protein Atlas consortium repository (www.proteinatlas.org) (28,29). Gene Expression Omnibus (GEO) datasets and profiles were downloaded directly from the National Center for Biotechnology Information / National Institutes of Health (NCBI/NIH). We collected gene-specific annotations and summary data from GeneCards (www.genecards.org), Human Base (http://hb.flatironinstitute.org) for human entries, and Mouse Genome Informatics (MGI; www.informatics.jax.org) for murine entries. Gene expression in response to IFN treatment in human hepatocyte cells (Huh7), human lung epithelial cells (A549), mouse embryonic fibroblasts (MEFs), and bone marrow-derived macrophages (BMDMs) was obtained from the Interferome database (www.interferome.org) and supplemented with published microarray matrices from previous studies (30–32). Microarray data of mouse RAW 264.7 macrophages stimulated with IFN-γ for 4 hours were retrieved from our published data files (33). We compiled transcriptomic datasets detailing human lung cell lines infected with respiratory viruses, mice challenged with the reconstructed 1918 influenza virus, and clinical patient samples from COVID-19 cohorts from prior reports (34–38). The GEO series accession numbers identifying human lung epithelial cells infected with SARS-CoV-2 and MERS-CoV included GSE147507, GSE148729, GSE79458, and GSE47961. We downloaded raw and processed microarray files spanning the GEO series from NCBI. We interrogated transcriptome responses driven by the TLR3 ligand poly(I: C) and the TLR4 ligand lipopolysaccharide (LPS) in mouse BMDMs and lung tissues from published datasets (39–42). We retrieved differential expression profiles from the GEO datasets using the GeoR2R method (NCBI/NIH, USA), relying on biological triplicate data points per experimental condition. We performed hierarchical cluster analysis across linked arrays and co-regulated genes using the Heatmapper expression software package (43). We also used resources from the Immunological Genome Project (ImmGen) for data analysis.

3 Results and Discussion

3.1 Identification of PLEKHA4 as a Hub in the Interferon-Mediated Antiviral Signaling Network

Transcription factor profiling of immune and lung epithelial cell transcriptomes has revealed that type I interferon signaling comprises several inducible transcription factor sub-networks, including antiviral response, cell growth, and immune modulation (15,16). The core set of inducible transcription factors involved in the type I interferon-induced antiviral response includes *ST*AT1, STAT2, IRF1, IRF5, IRF7, IRF9, SP100, SP110, NMI, and PML (15). Although several antiviral zinc-finger transcription factors such as ZCCHC2 and ZC3HAV1 were induced by type I interferons in different cell types, we only included ZCCHC2 in this study (15,16).

Visualization of transcription factors involved in core type I interferon signaling using the STRING database revealed multiple interactions among STAT and IRF family members alongside other inducible transcription factors (Figure 1A). Signaling molecules, such as transcription factors involved in related biological functions, often share common protein interaction partners and target genes (18). Pairwise comparison of common interaction partners of critical hubs (PIC-Venn) combined with differential gene expression analysis has previously identified novel signaling molecules, critical nodes, and network modules (18). Applying the PIC-Venn method to STAT1 and other core components of type I interferon signaling demonstrated that several additional proteins participate in the antiviral response network (Figure 1B and Table 1). These include established signaling hubs in immune response and type I interferon signaling, such as STAT3, MAVS, and BRCA1 (18,44,45). Intersection analysis of interaction partners associated with critical hubs (STAT1, STAT2, and PML) revealed several novel candidate hubs (Figure 2):

1. ESR2 (Estrogen receptor 2): Involved in estrogen-responsive gene (ERG) regulation (46).

2. FBXW7 (F-box/WD repeat-containing protein 7): Involved in ubiquitination (47).
3. SMARCA4/BRG1 (SWI/SNF-related matrix-associated actin-dependent regulator of chromatin subfamily A member 4): Possesses helicase and ATPase activities involved in chromatin remodeling (48,49,50).
4. PLEKHA4 (Pleckstrin homology domain-containing family A member 4): Involved in cell signaling, lipid metabolism, and membrane dynamics (19,20).

Among these hubs, SMARCA4/BRG1 regulates chromatin remodeling at STAT1 and CIITA target genes during interferon-gamma (IFN-γ) signaling, as well as STAT3 target genes during interleukin-6 (IL-6) signaling (48–50). The BioGRID database reports an interaction between ESR2 and STAT1, but the functional consequences remain to be established. PLEKHA4 serves as a common hub for STAT1/STAT2/PML interaction partners, suggesting a functional role in type I interferon signaling (Figure 2). PubMed metadata analysis indicated that PLEKHA4 was studied for its role in developmental pathways, Wnt and Phosphoinositide signaling, and oncogenesis (19,20; summarized in Figure 3). However, its role in interferon signaling remains unclear. For these reasons, we selected PLEKHA4 for detailed bioinformatic and functional characterization. Metascape enrichment analysis revealed that PLEKHA4 is associated with Gene Ontology (GO) terms related to cytokine signaling (IL-6, IL-20) and host responses to respiratory viruses, such as influenza. Network mapping showed that PLEKHA4 interacts with multiple members of the type I interferon antiviral sub-network (Figures 4A and 4B). Data from BioGRID revealed that several antiviral hubs co-expressed with PLEKHA4, specifically STAT1, STAT3, PML, and SMARCA4, all share binding interactions with AKT1. This overlap suggests that PLEKHA4 might modulate the PI3K/AKT signaling pathway during interferon responses. Protein interactions between PLEKHA4 and STAT3 may modulate IL-6 signaling pathways in inflammatory diseases and cancer. Functional enrichment in human

disease networks linked PLEKHA4 and its antiviral protein interaction partners to oncogenesis, mycobacterial infections, and Respiratory Syncytial Virus (RSV) disease (Supplementary Figure 1).

3.2 Tissue- and Cell-Specific Expression of PLEKHA4

A gene's biological functions often correlate with its tissue- and cell-specific expression profiles across organisms (51). Therefore, we analyzed PLEKHA4 expression in the Genotype-Tissue Expression (GTEx) database to gain insights into its physiological roles (28). PLEKHA4 was highly expressed in human female reproductive tissues (ovary, breast, and uterus) and male reproductive tissues (testis and prostate), suggesting sex hormone regulation in these organs (Figure 5).

The highest PLEKHA4 expression was detected in tibial nerve tissue (Figure 5). Analysis of the ImmGen database revealed that among immune organs, PLEKHA4 was prominently expressed in medullary thymic epithelial cells and lymph nodes (data not shown). High-resolution transcriptomic data from the Human Protein Atlas (HPA) and GTEx databases indicate that PLEKHA4 is expressed in both lung and liver tissues. These organs serve as primary targets for major respiratory and hepatic pathogens, including influenza and hepatitis C virus (HCV) (1,52).

The lung is a complex structural organ composed of epithelial, fibroblast, and endothelial cells (53). Single-cell expression mapping in the HPA database revealed that PLEKHA4 transcript levels are significantly higher in lung fibroblasts, with lower levels present in AT2 alveolar cells, club cells, ciliated cells, and endothelial cells. Resident immune populations such as T cells and alveolar macrophages showed very low baseline expression (Figure 6). This cell-specific distribution could shape local immune responses during viral infection. For example, seasonal influenza tends to be restricted to upper airways, whereas lethal strains like the 1918 H1N1 virus invade distal lung tissue to trigger extensive immunopathology (1,37).

Although human hepatocytes express low basal levels, interferon stimulation strongly upregulates PLEKHA4, which may help orchestrate the antiviral program in the liver. Based on sequence annotations in the MGI and HPA repositories, PLEKHA predominantly localizes to the extracellular space or the inner leaflet of the plasma membrane.

3.3 Differential Expression of PLEKHA4 in HCV-Permissive and Non-Permissive Hepatoma Cells

In vitro studies of hepatitis C virus (HCV) replication frequently utilize Huh-7 hepatoma models (52,54). Parental Huh-7 cells show low permissiveness to HCV, unlike susceptible derivatives like Huh-7.5.1 and HRP-1 (52). Susceptibility depends on a balance of host factors - entry receptors (CD81, SR-BI, CLDN1) and antiviral restriction proteins like IFITM1(52). Innate immunity driven by type I interferons strongly restricts viral proteins (including NS5A) through effector induction, while microRNA-122 and tumor suppressor TP53 further modulate viral output (52,55–57). Interestingly, PLEKHA4 transcript levels were suppressed in HCV-permissive lines compared to their non-permissive parent cells (Figure 7).

3.4 Regulation of PLEKHA4 by Type I, Type II, and Type III Interferons

Gene expression data from the GEO and Interferome databases showed that type I IFNs regulate PLEKHA4 in hepatocytes, fibroblasts, macrophages, and lung epithelial cells of humans and mice (Figure 8 and Figure 9). PLEKHA4 was strongly upregulated in human hepatocytes and mouse embryonic fibroblast cells by 8–30-fold (Figure 8A). Expression was rapid (within 4–6 hours) in human cells and remained elevated for 18–24 hours (Figure 8A–8C). PLEKHA4 expression was specifically activated by type I IFNs (IFN-α, IFN-β) but not by type III IFN (IFN-λ) in Huh-7 cells (Figure 8B). Both type I and type II IFNs (IFN-γ) activated PLEKHA4 expression in mouse embryonic fibroblasts (data not shown). A549 lung epithelial cells are commonly used as a model system to study innate immune responses to respiratory pathogens (34,35).

PLEKHA4 was co-expressed with other classic ISGs (IFIT1, IFIT2, OAS1, and OAS2) following IFN treatment. Expression levels were enhanced by 6 hours and remained elevated up to 24 hours post-treatment (Figure 8C). IFN-γ treatment of RAW264.7 mouse macrophages led to strong induction of ISGs within 4 hours of treatment (Figure 9A). PLEKHA4 was also upregulated alongside several antiviral transcription factors in Huh-7 hepatoma cells (Figure 9B).

Interferon-regulated genes contain clusters of transcription factor binding sites within ISG promoters and enhancers (6). Type I IFN signaling can activate canonical ISRE-dependent and -independent promoters (15, 30). Examples of ISRE-dependent genes include CXCL10, OAS2, and STAT1, whereas ISRE-independent genes include NAMPT, CFB, TLR3, and PLEKHA4. Time-course analysis showed both gene groups had similar induction profiles (Figure 9B). The rapid, sustained increase in PLEKHA4 mRNA suggests cooperation between early phosphorylation-dependent STAT1 activation and downstream IFN-inducible transcription factors to maintain expression (Figure 9B).

Genomic analysis of the PLEKHA4 promoter region showed highly conserved STAT1 and IRF7 cis-elements directly downstream of the transcription start site (TSS) in human and mouse genes (Figure 10A). Mouse Plekha4 contained additional binding sites for Stat1 and Irf7 approximately 1,500 bp and 500 bp upstream of the TSS, respectively. This could potentially contribute to the stimulus-specific transcriptional response in murine cells. Mutant fibrosarcoma cell lines lacking key components of the JAK-STAT signaling were used in IFN-dependent pathway analysis (5, 58, 59). The parental 2fTGH cell line (wild-type) and U3A/U3C cell lines that lack STAT1 are well established for genetic reconstitution studies (60). IFN-α treatment strongly induced ISGs in 2fTGH cells (Figure 10B). Genetic reconstitution of the U3C cell line with wild-type STAT2 (U3C-STAT2 high) restored CXCL10, OAS2, and IFIT2 expression and antiviral response, confirming that a STAT1-independent and STAT2-dependent pathway is responsible for

induction of a subset of ISGs in human fibrosarcoma cells (Figure 10B). IFN-α treatment induced PLEKHA4 in 2fTGH cells but not in U3C-STAT2 cells, showing that its expression absolutely requires STAT1 (Figure 10B). IFN-α-induced activation of IRF7 RNA expression was lost in Huh-7 human hepatoma cells ; however, STAT1, STAT2, and PLEKHA4 RNA expression was maintained (Figure 10C). Similar results were obtained in cells treated with IFN-β (Figure 10C). These results indicate that type I IFN signaling regulates PLEKHA4 expression via a STAT1-dependent, IRF7-independent mechanism.

3.5 Regulation of PLEKHA4 Expression by Toll-Like Receptor (TLR) Ligands

Pathogen-associated molecular patterns (PAMPs) such as bacterial lipopolysaccharides (LPS) and viral double-stranded RNA (poly(I: C)) trigger responses in immune and lung epithelial cells via TLR4 and TLR3, respectively (61). TLR-mediated direct toxicity in conjunction with host inflammatory responses causes acute lung injury (ALI) (40,42). Secondary bacterial infection is common in patients with viral illness, exacerbating tissue damage (62,63). This is demonstrated by the presence of bacterial LPS in the blood of patients with severe COVID-19 (64). Intratracheal administration of LPS or poly(I: C) is commonly used in mice to mimic ALI pathology, identify signaling pathways, and investigate new treatments (40,42,65). TLR activation induces signal transduction pathways resulting in secretion of type I interferons, pro-inflammatory cytokines, and chemokines. Secreted interferons induce ISG expression in nearby tissues via an autocrine and paracrine route (5,6).

Analysis of GEO datasets revealed ISG gene expression varied depending on poly(I: C) concentration and treatment duration (39). Multiple type I IFN-regulated genes such as Cxcl9, Ifit2, Oas2, and Plekha4 were significantly increased at both low concentrations and short treatment durations (Figure 11A). Chromatin modifications by histone acetyltransferases (HATs) and deacetylases (HDACs) are key regulatory steps in the TLR and IFN pathways (41,66-68). Exposure of wild-type BMDMs to LPS caused an increase in Stat1 and Plekha4 levels after 4 hours. However, in Hdac3-

deficient BMDMs, Stat1 expression was greatly reduced at baseline, and Plekha4 and ISG expression were completely suppressed upon LPS exposure (Figure 11B). Overall, this demonstrates that Hdac3 is required for Stat1-induced expression of Plekha4 in mouse BMDMs. Poly(I: C) or LPS can be administered directly to the trachea to mimic key features of ALI in mice. This treatment induces localized expression of type I IFNs and inflammatory cytokines in the lungs (40,42). Plekha4 was highly upregulated and co-expressed with antiviral ISGs in the lungs of LPS- or poly(I: C) treated mice (Figure 12A and 12B). Overall, these data demonstrate that Plekha4 is a transcriptomic marker of ALI. Targeting HDAC3 could be a viable strategy to reduce pulmonary inflammation (41).

3.6 Role of PLEKHA4 in Mycobacterium tuberculosis (Mtb) Pathogenesis

Mtb is an intracellular bacterium that infects alveolar macrophages, the main innate immune response in the lungs (69). RNA sequencing comparing different strains of Mtb showed that Plekha4, along with a cluster of ISGs, were upregulated in mouse BMDMs infected with virulent strains (70). Upon infection of host cells with highly pathogenic strains of Mtb, Plekha4 levels are significantly increased with several key ISGs and pro-inflammatory cytokines (69,70). Lipoarabinomannan is a key component of the Mtb cell wall and alters signaling in macrophages to enhance the survival of the bacterium (71). TLR2/TLR1 heterodimer recognition of LAM causes downstream signaling that promotes type I IFN, cytokine, and chemokine production (72,73).

Gene expression analysis in THP-1 macrophage cells demonstrated that LAM treatment significantly increased PLEKHA4 gene expression as well as genes involved in the host defense response (73; Figure 13). This suggests that PLEKHA4 is not only involved in viral infections but also in the host response to bacterial pathogenesis. While type I IFNs are vital to the initial stages of host defense, overactive IFN responses may hinder intracellular bacterial clearance, causing severe

tuberculosis (74,75). Understanding the relationship between regulatory molecules such as PLEKHA4 and type I IFN signaling will be key in designing novel host-targeted treatments.

3.7 Regulation of PLEKHA4 by Respiratory Viruses

Infections by respiratory viruses result in diverse clinical outcomes, ranging from mild upper respiratory tract symptoms (seasonal flu, rhinovirus) to life-threatening pneumonia (SARS-CoV-2, 1918 H1N1 influenza) (1,13,76). Disease severity in coronavirus cases varies considerably and is often heightened in patients with pre-existing cardiovascular or pulmonary conditions (77,78). Furthermore, these pathogens exhibit distinct host and tissue tropisms: RSV predominantly affects pediatric populations, whereas human parainfluenza viruses (HPIV) tend to cause severe illness in elderly or immunocompromised individuals (79,80).

Human lung epithelial cell lines such as NHBE, A549, and Calu-3 are widely used to investigate viral entry, tissue tropism, and host transcriptomic changes in high-throughput experiments (13,35). SARS-CoV-2 infection resulted in a modest 2- to 3-fold increase in PLEKHA4 RNA levels in Calu-3 within 24 hours (Figure 14A). In contrast, MERS-CoV infection triggers a far more pronounced 10- to 15-fold rise in PLEKHA4 expression in Calu-3 cells and fibroblasts, respectively (Figure 14B). Host surface proteins like angiotensin-converting enzyme 2 (ACE2) facilitate entry for SARS-CoV-2 (81). In contrast, interferon-stimulated PLEKHA4 expression may function as a host-mediated restriction mechanism by altering membrane-associated signaling, endocytosis, or lipid dynamics.

Infection with RSV or HPIV3 similarly induced high PLEKHA4 expression within 24 hours in A549 cells (Figure 15A). Gene expression profiling in HPIV1-infected A549 cells demonstrated that PLEKHA4 induction follows the transcriptional activation of IFNB1 and inducible transcription factors (Figure 15B). These responses remain tightly modulated by intrinsic viral attributes such as strain virulence and specific

protein activities (82–84). For example, wild-type influenza A virus (IAV) fails to stimulate IFNB1 production or elevate STAT1, STAT2, or IRF9 expression in normal human bronchial epithelial (NHBE) cells due to NS1-mediated inhibition (35,84). However, infecting these cells with NS1-deficient IAV mutants or highly pathogenic strains (such as the 1918 H1N1 virus) restores robust induction of IFNB1, key transcription factors, and downstream ISGs (1,84,85).

While cell culture systems enable high-throughput testing, animal models remain essential for capturing systemic immunopathology and the contribution of different cell types(86,87). Murine models infected with highly pathogenic respiratory viruses display dramatic production of type I IFNs and proinflammatory cytokines, including Il-1β, Tnf-α, and Ifn-γ (1,34,37,38). These cytokines activate key transcription factors (AP-1, NF-κB, STAT1) across endothelial and epithelial tissues, driving chemokine production and recruiting immune cells that can exacerbate lung damage (1,15,38). Furthermore, an unbalanced, hyper-inflammatory cytokine profile occurs in severe cases of COVID-19 (4,13). Microarray evaluation of mouse lung tissue 3 to 4 days post-infection with the reconstructed 1918 H1N1 virus revealed prominent upregulation of Plekha4, chemokines, and antiviral mediators relative to mock-infected controls (Figure 16A). A similar response pattern featuring inducible transcription factors (IRF9, STAT2, and STAT1) alongside Plekha4 appeared in an aerosol SARS-CoV-2 mouse model (Figure 16B), confirming that Plekha4 upregulation represents a broad, conserved host response to severe respiratory viral challenges.

4 Conclusion

Pairwise analysis of interaction partners of critical hubs in type I interferon signaling identified PLEKHA4 as a novel component in the antiviral network. PLEKHA4 is a phosphoinositide-binding protein induced by type I and type II interferons in both human and mouse tissues. TLR ligands and infection with pathogenic respiratory viruses that trigger type I interferon release consistently upregulate PLEKHA4 both

in vitro and *in vivo*. Furthermore, type I interferon regulates PLEKHA4 induction through a STAT1-dependent, IRF7-independent pathway. While the role of the PI-3-kinase/AKT pathway in interferon signaling is well established (88,89), the precise role of PLEKHA4 within this pathway remains to be determined. In summary, PLEKHA4 is a candidate biomarker for inflammatory stress, suggesting its potential utility in evaluating therapies for viral and bacterial respiratory diseases.

Author's statement

Conflicts of Interest Statement: The Author declares no conflicts of interest.

Ethics Statement: This research did not required ethical approval.

Financial Support: This research received no specific grant from any funding agency, commercial or nonprofit sectors.

REFERENCES

1.Kash JC, Tumpey TM, Proll SC, et al. Genomic analysis of increased host immune response and cell death responses induced by 1918 influenza virus. Nature. 2008, 443: 578-581.

2. Huang, C., Wang, Y., Li, X., et al. (2020).Clinical features of patients infected with 2019 novel coronavirus in Wuhan, China. The Lancet, 2020. 395, 497–506.

3. Clementi N, Ghosh S, De Santis M, Castelli M, Criscuolo E, Zanoni I, Clementi M, Mancini N. Viral Respiratory Pathogens and Lung Injury. Clin Microbiol Rev. 2021 Mar 31;34(3):e00103-20.

4. Lucas C, Wong P, Klein J, Castro TBR, Silva J, Sundaram M, et.al. Longitudinal analyses reveal immunological misfiring in severe COVID-19. Nature. 2020 Aug;584(7821):463-469.

5. Stark, G. R., Kerr, I. M., Williams, B. R., et al. How cells respond to interferons. (1998). Annu Rev Biochem; 67, 227-264.

6. Platanias, L. (2005). Mechanisms of Type I- and Type II-interferon-mediated signaling. Nature Rev Immunol, 5, 375-386.

7. Kohlmeier, J. E., Woodland, D. L. (2009). Immunity to respiratory viruses. Annu Rev Immunol, 27, 61-82.

8. Ramana CV, DeBerge MP, Kumar A, Alia CS, Durbin JE, Enelow RI. Inflammatory impact of IFN-γ in CD8+ T cell-mediated lung injury is mediated by both Stat1-dependent and -independent pathways. Am J Physiol Lung Cell Mol Physiol. 2015 Apr 1;308(7):L650-7.

9. García-Sastre A, Durbin RK, Zheng H, Palese P, Gertner R, Levy DE, Durbin JE. The role of interferon in influenza virus tissue tropism. J Virol. 1998 Nov;72(11):8550-8.

10. Zhang, Q., Bastard, P., Liu, Z., Le Pen, J., Moncada-Velez, M., et. al. (2020). Inborn errors of type I IFN immunity in patients with life-threatening COVID-19. Science, 370, eabd4570.

11. Pairo-Castineira, E., Clohisey, S., Klaric, L., Bretherick, A.D., et. al. (2020). Genetic mechanisms of critical illness in Covid-19. 45 Nature. 2021 Mar;591(7848):92-98.

12. Bastard, P., Rosen, L.B., Zhang, Q., Michailidis, E., et.al. (2020).Autoantibodies against type I IFNs in patients with life- threatening COVID-19. Science, 370(6515)

13. Blanco-Melo, D., Nilsson-Payant, B.E., Liu, W. C., Uhl, S., Hoagland, D., et. al. (2020). Imbalanced host response to SARS-CoV-2 drives development of COVID-19. Cell, 181, 1036-1045.e9.

14. Ramana CV, Chatterjee-Kishore M, Nguyen H, Stark GR. Complex roles of Stat1 in regulating gene expression. Oncogene. 2000 May 15;19(21):2619-27.

15. Ramana C.V. and Das B (2021) Profiling transcription factor sub-networks in type I interferon signaling and in response to SARS-CoV-2 infection. Comput. Math. Biophys. 2021; 9:273–288.

16. Ramana C.V. and Das B (2021) Regulation of early growth response-1 (Egr-1) gene expression by Stat1-independent type I interferon signaling and respiratory viruses. Comput. Math. Biophys. 2021; 9:289–303.

17. Thorner J, Hunter T, Cantley LC, Sever R. Signal transduction: From the atomic age to the post-genomic era. Cold Spring Harb Perspect Biol. 2014; 6:a022913.

18. Ramana CV. Insights into functional connectivity in mammalian signal transduction pathways by pairwise comparison of protein interaction partners of critical signaling hubs. Biomol Concepts. 2022 Sep 1;13(1):298-313..

19. Shami Shah A, Batrouni AG, Kim D, Punyala A, Cao W, Han C, Goldberg ML, Smolka MB, Baskin JM. PLEKHA4/kramer Attenuates Dishevelled Ubiquitination to modulate Wnt and Planar Cell Polarity Signaling. Cell Rep. 2019 May 14;27(7):2157-2170.e8.

20. Yue Y, An G, Cao S, Li X, Du L, Xu D, Liu L. PLEKHA4 knockdown induces apoptosis in melanoma cells through the MAPK and β-catenin signaling pathways. Mol Med Rep. 2025 Apr;31(4):99.

21.Stark,C.,Breitkreutz,B.J.,Reguly,T.,Boucher,L.,Breitkreutz,A.,Tyers,M.(2006).BIOGRID:ageneralrepository forinter- action datasets. Nucleic Acids Res, 34, D535-D539.

22. Szklarczyk, D., Morris, J.H., Cook, H., Kuhn, M., et. al. (2017). The STRING database in 2017. Quality-controlled protein- protein association networks, made broadly accessible. Nucleic Acids Res. 45:D362-D368.

23. Orii, N., and Ganapathiraju, M. K. (2012). WIKI-PI: a web server of annotated human protein-protein interactions to aid in discovery of protein function. PLoS One, 7, e49029.

24. Huang da, W., Sherman, B. T., Lempicki, R. A. (2009). Systematic and integrative analysis of large gene lists using DAVID bioinformatics resources. Nat Protoc, 4(1), 44.

25. Zhou, Y., Zhou, B., Pache, L., Chang, M., et.al.(2019). Metascape provides a biologist-oriented resource for the analysis of systems-level datasets. Nat Commun, 10, 1523.

26. Kanehisa, M., Furumichi, M., Tanabe, M., Sato, Y., Morishima, K. (2017). KEGG: new perspectives on genomes, pathways, diseases and drugs. Nucleic Acids Res, 45, D353-D361.

27. Han H, Cho JW, Lee S, Yun A, Kim H, Bae D, Yang S, Kim CY, Lee M, Kim E, Lee S, Kang B, Jeong D, Kim Y, Jeon HN, Jung H, Nam S, Chung M, Kim JH, Lee I. TRRUST v2: an expanded reference database of human and mouse transcriptional regulatory interactions. Nucleic Acids Res. 2018; 46:D380-D386.

28. The GTEx Consortium atlas of genetic regulatory effects across human tissues. The GTEx Consortium. Science. 369 (1318-1330), 10 Sep 2020. doi:10.1126/science.aaz1776

29. Thul, P. J. et al. A subcellular map of the human proteome. Science 356, eaal3321 (2017).

30. Rusinova I, Forster S, Yu S, Kannan A, Masse M, Cumming H, Chapman R, Hertzog PJ. Interferome v2.0: an updated database of annotated interferon-regulated genes. Nucleic Acids Res. 2013 Jan;41(Database issue): D1040-6.

31. Bolen CR, Ding S, Robek MD, Kleinstein SH. Dynamic expression profiling of type I and type III interferon-stimulated hepatocytes reveals a stable hierarchy of gene expression. Hepatology. 2014 Apr;59(4):1262-72.

32. Boonyaratanakornkit JB, Bartlett EJ, Amaro-Carambot E, Collins PL, Murphy BR, Schmidt AC. The C proteins of human parainfluenza virus type 1 (HPIV1) control the transcription of a broad array of cellular genes that would otherwise respond to HPIV1 infection. J Virol. 2009 Feb;83(4):1892-910.

33. Kota RS, Rutledge JC, Gohil K, Kumar A, Enelow RI, Ramana CV. Regulation of gene expression in RAW 264.7 macrophage cell line by interferon-gamma. Biochem Biophys Res Commun. 2006 Apr 21;342(4):1137-46.

34. Nilsson-Payant BE, Uhl S, Grimont A, Doane AS, Cohen P, Patel RS, Higgins CA, Acklin JA, Bram Y, Chandar V, Blanco-Melo D, Panis M, Lim JK, Elemento O, Schwartz RE, Rosenberg BR, Chandwani R, tenOever BR. The NF-κB Transcriptional Footprint Is Essential for SARS-CoV-2 Replication. J Virol. 2021 Nov 9;95(23):e0125721.

35. Wyler E, Mösbauer K, Franke V, Diag A, et al. Transcriptomic profiling of SARS-CoV-2 infected human cell lines identifies HSP90 as target for COVID-19 therapy. iScience. 2021;24(3):102151.

36. Daamen AR, Bachali P, Owen KA, Kingsmore KM, et al. Comprehensive transcriptomic analysis of COVID-19 blood, lung, and airway. Sci Rep. 2021;11(1):7052.

37. Walters KA, D'Agnillo F, Sheng ZM, Kindrachuk J, Schwartzman LM, Kuestner RE, Chertow DS, Golding BT, Taubenberger JK, Kash JC. 1918 pandemic influenza virus and Streptococcus pneumoniae co-infection results in activation of coagulation and widespread pulmonary thrombosis in mice and humans. J Pathol. 2016;238(1):85-97.

38. Fumagalli V, Ravà M, Marotta D, Di Lucia P, Laura C, Sala E, Grillo M, Bono E, Giustini L, Perucchini C, Mainetti M, Sessa A, Garcia-Manteiga JM, Donnici L, Manganaro L, Delbue S, Broccoli V, De Francesco R, D'Adamo P, Kuka M, Guidotti LG, Iannacone M. Administration of aerosolized SARS-CoV-2 to K18-hACE2 mice uncouples respiratory infection from fatal neuroinvasion. Sci Immunol. 2022; 7(67):eabl9929.

39. Gold ES, Diercks AH, Podolsky I, Podyminogin RL, Askovich PS, Treuting PM, Aderem A. 25-Hydroxycholesterol acts as an amplifier of inflammatory signaling. Proc Natl Acad Sci U S A. 2014 Jul 22;111(29):10666-71.

40. Harris P, Sridhar S, Peng R, Phillips JE, et al. Double-stranded RNA induces molecular and inflammatory signatures that are directly relevant to COPD. Mucosal Immunol 2013;6(3):474-84

41. Chen X, Barozzi I, Termanini A, Prosperini E, Recchiuti A, Dalli J, Mietton F, Matteoli G, Hiebert S, Natoli G. Requirement for the histone deacetylase Hdac3 for the inflammatory gene expression program in macrophages. Proc Natl Acad Sci U S A. 2012 Oct 16;109(42): E2865-74.

42. Britto CJ, Niu N, Khanal S, Huleihel L, Herazo-Maya JD, Thompson A, Sauler M, Slade MD, Sharma L, Dela Cruz CS, Kaminski N, Cohn LE. BPIFA1 regulates lung neutrophil recruitment and interferon signaling during acute inflammation. Am J Physiol Lung Cell Mol Physiol. 2019;316(2):L321-L333.

43. Babicki S, Arndt D, Marcu A, Liang Y, Grant JR, Maciejewski A, Wishart DS. Heatmapper: web-enabled heat mapping for all. Nucleic Acids Res. 2016; 44(W1): W147-53.

44. Tsai, M.H., Pai, L.M., Lee, C.K. (2019). Fine-tuning of Type I Interferon response by STAT3. FrontImmunol,10,1448.

45. Ren Z, Ding T, Zuo Z, Xu Z, Deng J, Wei Z. Regulation of MAVS Expression and Signaling Function in the Antiviral Innate Immune Response. Front Immunol. 2020 May 27;11:1030.

46. Hamilton KJ, Hewitt SC, Arao Y, Korach KS. Estrogen Hormone Biology. Curr Top Dev Biol. 2017;125:109-146.

47. He J, Du Y, Li G, Xiao P, Sun X, Song W, Lai L, Xia M, Zhang J, Wang Q. Myeloid Fbxw7 Prevents Pulmonary Fibrosis by Suppressing TGF-β Production. Front Immunol. 2022 Jan 5;12:760138.

48. Zhang Y, Cheng MB, Zhang YJ, Zhong X, Dai H, Yan L, Wu NH, Zhang Y, Shen YF. A switch from hBrm to Brg1 at IFNγ-activated sequences mediates the activation of human genes. Cell Res. 2010 Dec;20(12):1345-60.

49. Ni Z, Abou El Hassan M, Xu Z, Yu T, Bremner R. The chromatin-remodeling enzyme BRG1 coordinates CIITA induction through many interdependent distal enhancers. Nat Immunol. 2008 Jul;9(7):785-93.

50. Ni Z, Bremner R. Brahma-related gene 1-dependent STAT3 recruitment at IL-6-inducible genes. J Immunol. 2007 Jan 1;178(1):345-51.

51. Yuan F, Pan X, Zeng T, Zhang YH, Chen L, Gan Z, Huang T, Cai YD. Identifying Cell-Type Specific Genes and Expression Rules Based on Single-Cell Transcriptomic Atlas Data. Front Bioeng Biotechnol. 2020 Apr 29;8:350.

52. MacPherson JI, Sidders B, Wieland S, Zhong J, Targett-Adams P, Lohmann V, Backes P, Delpuech-Adams O, Chisari F, Lewis M, Parkinson T, Robertson DL. An integrated transcriptomic and meta-analysis of hepatoma cells reveals factors that influence susceptibility to HCV infection. PLoS One. 2011;6(10):e25584.

53. Maeda Y, Dave V, Whitsett JA. Transcriptional control of lung morphogenesis. Physiol Rev. 2007;87:219–244.

54. Lohmann V, Körner F, Koch J, Herian U, Theilmann L, Bartenschlager R. Replication of subgenomic hepatitis C virus RNAs in a hepatoma cell line. Science. 1999 Jul 2;285(5424):110-3.

55. Samreen B, Khaliq S, Ashfaq UA, Khan M, Afzal N, Shahzad MA, Riaz S, Jahan S. Hepatitis C virus entry: role of host and viral factors. Infect Genet Evol. 2012 Dec;12(8):1699-709.

56. Milosevic I, Todorovic N, Filipovic A, Simic J, Markovic M, Stevanovic O, Malinic J, Katanic N, Mitrovic N, Nikolic N. HCV and HCC Tango-Deciphering the Intricate Dance of Disease: A Review Article. Int J Mol Sci. 2023 Nov 7;24(22):16048.

57. Kunden RD, Khan JQ, Ghezelbash S, Wilson JA. The Role of the Liver-Specific microRNA, miRNA-122 in the HCV Replication Cycle. Int J Mol Sci. 2020 Aug 7;21(16):5677.

58. Brabant D, Michael P, Bleiblo F, Saleh M, Narain R, Tai TC, Ramana CV, Parrillo JE, Kumar A, Kumar A. Septic sera induces apoptosis and DNA fragmentation factor 40 activation in fibroblasts. Biochem Biophys Res Commun. 2011 Aug 26;412(2):260-5.

59. Bleiblo F, Michael P, Brabant D, Ramana CV, Tai T, Saleh M, Parrillo JE, Kumar A, Kumar A. JAK kinases are required for the bacterial RNA and poly I: C-induced tyrosine phosphorylation of PKR. Int J Clin Exp Med. 2013;6(1):16-25.

60.Blaszczyk K, Olejnik A, Nowicka H, Ozgyin L, Chen YL, Chmielewski S, Kostyrko K, Wesoly J, Balint BL, Lee CK, Bluyssen HA. STAT2/IRF9 directs a prolonged ISGF3-like transcriptional response and antiviral activity in the absence of STAT1. Biochem J. 2015 Mar 15;466(3):511-24.

61. Kumar H, Kawai T, Akira S. Pathogen recognition by the innate immune system. Int Rev Immunol. 2011; 30(1):16-34.

62. Hanada, S.; Pirzadeh, M.; Carver, K.Y.; Deng, J.C. Respiratory Viral Infection-Induced Microbiome Alterations and Secondary Bacterial Pneumonia. Front. Immunol. 2018, 9, 2640.

63. Kalil AC, Thomas PG. Influenza virus-related critical illness: pathophysiology and epidemiology. Crit Care. 2019 Jul 19;23(1):258.

64. Arunachalam PS, Wimmers F, Mok CKP, Perera RAPM, Scott M, Hagan T, Sigal N, Feng Y, Bristow L, Tak-Yin Tsang O, Wagh D, Coller J, Pellegrini KL, Kazmin D, et al. Systems biological assessment of immunity to mild versus severe COVID-19 infection in humans. Science. 2020 Sep 4;369(6508):1210-1220

65. Beutler, B. LPS in microbial pathogenesis: Promise and fulfillment. J. Endotoxin Res. 2002, 8, 329–335.

66. Zhuang S. Regulation of STAT signaling by acetylation. Cell Signal. 2013 Sep;25(9):1924-31.

67. Nusinzon I, Horvath CM. Interferon-stimulated transcription and innate antiviral immunity require deacetylase activity and histone deacetylase 1. Proc Natl Acad Sci U S A. 2003 Dec 9;100(25):14742-7.

68. Mishra B, Ivashkiv LB. Interferons and epigenetic mechanisms in training, priming and tolerance of monocytes and hematopoietic progenitors. Immunol Rev. 2024 May;323(1):257-275.

69. Chai Q, Wang L, Liu CH, Ge B. New insights into the evasion of host innate immunity by Mycobacterium tuberculosis. Cell Mol Immunol. 2020 Sep;17(9):901-913.

70. Leisching G, Pietersen RD, van Heerden C, van Helden P, Wiid I, Baker B. RNAseq reveals hypervirulence-specific host responses to M. tuberculosis infection. Virulence. 2017 Aug 18;8(6):848-858.

71. Correia-Neves M, Sundling C, Cooper A, Källenius G. Lipoarabinomannan in Active and Passive Protection Against Tuberculosis. Front Immunol. 2019 Sep 11;10:1968.

72. Oliveira-Nascimento L, Massari P, Wetzler LM. The Role of TLR2 in Infection and Immunity. Front Immunol. 2012 Apr 18;3:79.

73. Halder P, Kumar R, Jana K, Chakraborty S, Ghosh Z, Kundu M, Basu J. Gene expression profiling of Mycobacterium tuberculosis Lipoarabinomannan-treated macrophages: A role of the Bcl-2 family member A1 in inhibition of apoptosis in mycobacteria-infected macrophages. IUBMB Life. 2015 Sep;67(9):726-36.

74. Olson GS, Murray TA, Jahn AN, Mai D, Diercks AH, Gold ES, Aderem A. Type I interferon decreases macrophage energy metabolism during mycobacterial infection. Cell Rep. 2021 Jun 1;35(9):109195.

75. Moreira-Teixeira L, Mayer-Barber K, Sher A, O'Garra A (2018) Type I interferons in tuberculosis: foe and occasionally friend. J Exp Med 215(5):1273–1285

76. To KKW, Yip CCY, Yuen KY. Rhinovirus - From bench to bedside. J Formos Med Assoc. 2017 Jul;116(7):496-504.

77. Ko JY, Danielson ML, Town M, Derado G, et. al. COVID-NET Surveillance Team. Risk Factors for Coronavirus Disease 2019 (COVID-19)-Associated Hospitalization: COVID-19-Associated Hospitalization Surveillance Network and Behavioral Risk Factor Surveillance System. Clin Infect Dis. 2021 Jun 1;72(11):e695-e703

78. Grasselli G, Tonetti T, Protti A, Langer T, et. al. Pathophysiology of COVID-19-associated acute respiratory distress syndrome: a multi-centre prospective observational study. Lancet Respir Med. 2020 Dec;8(12):1201-1208.

79. Borchers AT, Chang C, Gershwin ME, Gershwin LJ. Respiratory syncytial virus--a comprehensive review. Clin Rev Allergy Immunol. 2013 Dec;45(3):331-79.

80. Henrickson KJ. Parainfluenza viruses. Clin Microbiol Rev. 2003 Apr;16(2):242-64.

81. Hoffmann M, Kleine-Weber H, Schroeder S, Krüger N, Herrler T, Erichsen S, Schiergens TS, Herrler G, Wu NH, Nitsche A, Müller MA, Drosten C, Pöhlmann S. SARS-CoV-2 Cell Entry Depends on ACE2 and TMPRSS2 and Is Blocked by a Clinically Proven Protease Inhibitor. Cell. 2020 Apr 16;181(2):271-280.e8. 7.

82. Liang Y. Pathogenicity and virulence of influenza. Virulence. 2023 Dec;14(1):2223057.

83. Michael P, Brabant D, Bleiblo F, Ramana CV, Rutherford M, Khurana S, Tai TC, Kumar A, Kumar A. Influenza A- induced cellular signal transduction pathways. J Thorac Dis. 2013;5 Suppl 2:S132-41.

84. Han CW, Jeong MS, Jang SB. Structure and Function of the Influenza A Virus Non-Structural Protein 1. J Microbiol Biotechnol. 2019; 29(8):1184-1192.

85. Ramana, C. V. and Das, B. Regulation of Lysosomal Associated Membrane Protein 3 (LAMP3) in Lung Epithelial Cells by Coronaviruses (SARS-CoV-1/2) and Type I Interferon Signaling. Computational and Mathematical Biophysics, vol. 10, no. 1, 2022, pp. 167-183.

86. Kirk NM, Liang Y, Ly H. Comparative Pathology of Animal Models for Influenza A Virus Infection. Pathogens. 2023 Dec 29;13(1):35.

87. Dillard JA, Martinez SA, Dearing JJ, Montgomery SA, Baxter VK. Animal Models for the Study of SARS-CoV-2-Induced Respiratory Disease and Pathology. Comp Med. 2023 Feb 1;73(1):72-90.

88. Nguyen H, Ramana CV, Bayes J, Stark GR. Roles of phosphatidylinositol 3-kinase in interferon-gamma-dependent phosphorylation of STAT1 on serine 727 and activation of gene expression. J Biol Chem. 2001 Sep 7;276(36):33361-8.

89. Kaur S, Uddin S, Platanias LC. The PI3K kinase pathway in interferon signaling. J Interferon Cytokine Res. 2005 Dec;25(12):780-7.

Table 1. PIC-VENN analysis of inducible transcription factors in core type I interferon signaling

STAT1vs IRF9	STAT1vs IRF5	STAT1vs IRF7	STAT1vs IRF1	STAT1vs STAT2	STAT1vs PML	STAT1vs NMI	STAT1vs ZCCHC2	PIC-VENN
STAT2	CREBBP	IRAK1	EP300	CREBBP	UBE2I	BRCA1	HUWE1	MYC
IRF1	EP300	TRIM28	TRIM28	EP300	RNF4	MYC	MYC	BRCA1
STAT1	HDAC1	CREBBP	IRF9	IFNAR2	HDAC1	STAT5A	OTUD4	UBE2I
CREBBP	MAVS	EP300	CREBBP	KPNA1	CREBBP	UBE2I		RELA
IFNAR2	COPS5	MAVS	FBXW7	SMARCA4	JUN	APEH		STAT1
RELA		NMI	SMARCA4	IRF9	MYC	HSPA8		STAT3
		RNF31		PARP9	CTNNB1	NAA10		CREBBP
		TNFAIP3		PML	EGFR	RELA		HDAC1
				XPO1	HDAC3	STAT1		EGFR
				CDH1	PIAS1	STAT3		JAK1
				EGFR	RELA	TBCD		ESR2
				ESR2	RXRA	VPS26A		EP300
				FBXW7	STAT1			PLEKHA4
				GSK3A	STAT3			SMARCA4
				PLEKHA4	JAK1			STAT2
				JAK1	BRCA1			FBXW7
				JAK2	BRD4			IRF9
					ESR2			IFNAR2
					FOS			TRIM28
					MTOR			MAVS
					HIPK2			
					NTRK1			
					PER2			
					PLEKHA4			
					PPARG			
					SMARCA4			
					STAT2			
					YAP1			
					E2F1			
					TES			

(Common interaction partners of several critical hubs of type I Interferon signaling revealed by pairwise comparison)

Figure legends

Figure 1. Protein-protein interactions of transcription factors in the antiviral sub-network in the core type I interferon signaling.

(A) Transcription factors were represented by ovals and protein interactions by edges in the STRING database. (B) Pairwise matrix analysis of protein interaction partners of critical hubs in the antiviral sub-network of the core type I interferon signaling.

Figure 2. Venn diagram of interaction partners that are common to critical hubs STAT1, STAT2, and PML in WIKI-PI and BIOGRID databases.

Common interacting partners between the two datasets were highlighted in bold letters. Venn diagrams were represented using the Intervene Shiny app.

Figure 3. Signal transduction pathways and biological processes associated with PLEKHA4.

Signal transduction pathways and biological processes associated with PLEKHA4 were retrieved from the Human Base website.

Figure 4. Annotation of biological functions and signal transduction pathways associated with antiviral signaling hubs revealed by PIC-Venn in type I interferon signaling.

(A) Gene ontology (GO) terms associated with the antiviral sub-network involving known and novel pathways induced by type I signaling were ranked by significance using Metascape software tools. (B) Analysis of the protein-protein interaction (PPI)network of known and novel hubs revealed by PIC-Venn in type I interferon signaling using STRING database tools. Transcription factors and critical hubs were represented by ovals and protein interactions by edges, respectively.

Figure 5. Tissue-specific expression of PLEKHA4 in human tissues.

PLEKHA4 RNA levels in different human tissues were retrieved from the GTEx database (Broad Institute). Transcripts per million (TPM) reads were indicated.

Figure 6. RNA expression levels of PLEKHA4 in different cell types of human lung tissue.

PLEKHA4 RNA levels in different cell types of human lung tissue were retrieved from the HPA database. RNA expression levels of PLEKHA4, along with cell-specific markers for lung AT1, AT2, Club, and Ciliated cells, were shown as a heatmap.

Figure 7. Differential expression of PLEKHA4 in HCV non-permissive and permissive hepatoma cells.

PLEKHA4 RNA expression levels in HUH-7 (non-permissive), HUH 7.5, and HRP1(permissive) cell lines for HCV replication were shown.

Figure 8. Regulation of PLEKHA4 RNA levels by interferon treatment in human and mouse cells.

(A) Time course regulation of PLEKHA4 RNA levels by IFN-α treatment in human hepatocytes and IFN-β treatment in mouse fibroblast cells. (B) Differential regulation of PLEKHA4 by IFN-α, IFN-β, or IFN-λ. Cells were treated for 6 h in Huh-7 hepatoma cells. (C) Time course of interferon-stimulated gene expression in A549 lung epithelial cells treated with IFN-β was shown using the Heatmapper software. Microarray data were retrieved from the Interferome and GEO datasets.

Figure 9. PLEKHA4 induction by interferons is correlated with inducible transcription factor expression in mouse and human cells.

(A) RAW264.7 mouse macrophages were treated with IFN-γ for 4 h, and RNA levels of interferon-stimulated genes and transcription factors were determined by microarray analysis. (B) Human hepatoma Huh-7 cells were treated with IFN-β for several hours, and RNA levels of interferon-stimulated genes and transcription factors were retrieved from the GEO dataset.

Figure 10. Regulation of PLEKHA4 by type I interferon is STAT1-dependent and IRF7-independent

(A) Schematic representation of the human (PLEKHA4) and mouse (Plekha4) gene promoter sequence elements retrieved from the Interferome database. The approximate locations of the STAT1 and IRF7 binding sites in the human and mouse gene promoters are shown. TSS represents the transcription start site. (B) Regulation of PLEKHA4 and interferon-stimulated genes in 2fTGH (wild-type) and Stat1-null (U3C) overexpressing STAT2 was shown at 8 and 24 h of IFN-α treatment. (C) Regulation of PLEKHA4 and interferon-induced transcription factors at RNA levels by IFN-β or IFN-α treatment for 6 h in Huh7 hepatocytes. Relative fold induction of transcription factors by interferon-β and interferon-α was shown by blue and red bars, respectively.

Figure 11. Regulation of PLEKHA4 and interferon-stimulated genes by TLR ligands in bone marrow-derived macrophages (BMDMs).

(A) BMDMs were treated with 6 or 18 μg of double-stranded RNA mimetic poly I: C for 6 or 18 h. (B) BMDMs from wild-type or HDAC3 KO mice were treated with LPS (100ng/ml) for 4 hours. RNA expression values were normalized and are shown as a heatmap

Figure 12. Regulation of PLEKHA4 and interferon-stimulated genes by TLR ligands in the lungs of mouse models of acute lung injury.

(A) Mice treated with vehicle (mock) or LPS via intratracheal instillation for 8 or 24 h. (B) Mice treated with vehicle (mock) or poly I: C via intratracheal instillation for 6, 12, or 24 h. RNA expression values were normalized and are shown as a heatmap.

Figure 13. Regulation of PLEKHA4 and interferon-stimulated genes by Mycobacterial Lipoarabinomannan (LAM) in THP-1 macrophage cells.

Expression levels of PLEKHA4 and interferon-stimulated genes in human macrophage cell line THP-1 cells treated with mycobacterial cell wall component Lipoarabinomannan (LAM).

Figure 14. Regulation of PLEKHA4 and interferon-stimulated genes (ISG) by Coronaviruses in lung epithelial cells.

(A) Regulation of PLEKHA4 RNA levels in response to mock or SARS-CoV-2 in Calu-3 lung epithelial cells. PLEKHA4 expression values were normalized by DESeq2, and data from three samples for each condition were shown. (B) Regulation of PLEKHA4 gene expression in response to MERS-CoV infection in Calu-3 lung epithelial cells and fibroblast cells..

Figure 15. Regulation of PLEKHA4 mRNA levels by respiratory syncytial virus (RSV) and human parainfluenza virus (HPIV).

(A) Human A549 lung cells were mock-infected or infected with RSV or HPIV3 for 24 h. PLEKHA4 mRNA levels were normalized and expressed as fold induction from triplicate samples. (B) Time course of PLEKHA4 and interferon-stimulated gene expression in response to HPIV1 infection in A549 lung epithelial cells

Figure 16. Regulation of RNA expression levels of Plekha4 in the mouse lungs by highly pathogenic respiratory viruses.

(A) Regulation of Plekha4 and interferon-stimulated antiviral response genes, inflammation regulators, and transcription factors at the RNA level in mouse lungs by the reconstructed 1918 H1N1 influenza virus. Mice were mock-infected or infected with the virus for 3 or 4 days. Heatmap representation of interferon-regulated gene expression. Data from three samples for each condition are shown. (**B**) Regulation of Plekha4 and interferon-regulated transcription factors at RNA levels in the lungs in an aerosol model of SARS-CoV-2 infection in mice.

Expression levels of the interferon-regulated genes were shown as fold induction compared with mock infection.

Supplementary Figure 1. Diseases associated with the antiviral sub-network of type I interferon signaling.

Figure 1

A

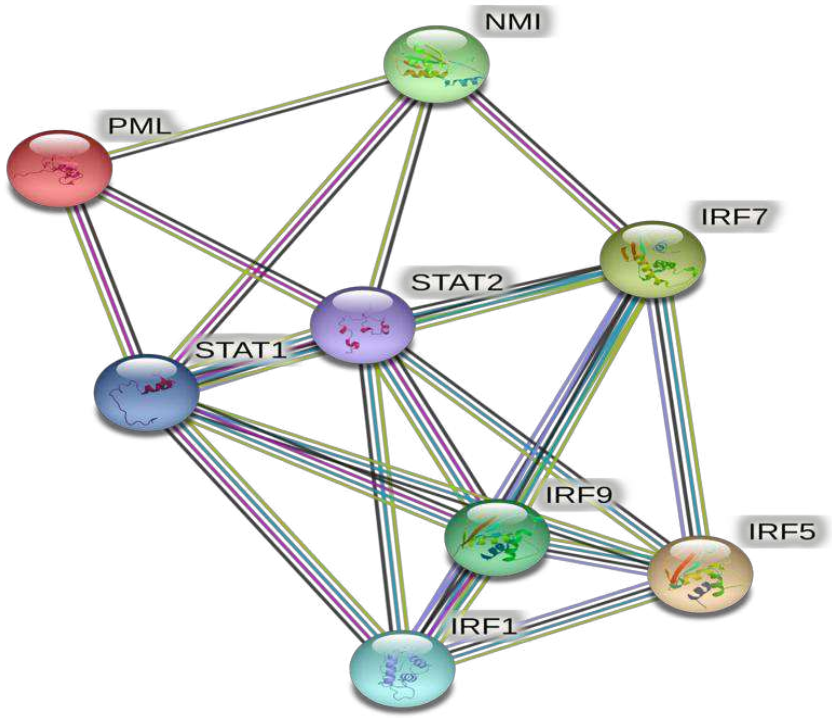

B

	STAT1	STAT2	IRF1	IRF5	IRF7	IRF9	PML	NMI
STAT1		17	6	5	8	6	30	12
STAT2	17		8	2	2	4	11	1
IRF1	6	8		5	8	2	7	1
IRF5	5	2	5		7	1	5	1
IRF7	8	2	8	7		1	6	4
IRF9	6	4	2	1	1		5	3
PML	30	11	7	5	6	5		9
NMI	12	1	1	1	4	3	9	

Figure 2

WIKI-PI database

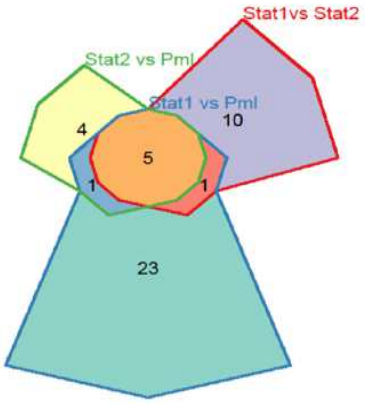

(CREBBP, JAK1 ,EGFR, SMARCA4, ESR2,PLEKHA4)

BIOGRID database

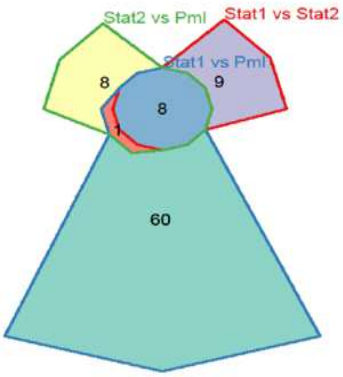

(CREBBP, JAK1 ,EGFR, SMARCA4, FBXW7, **ESR2,**PARP9, **PLEKHA4)**

Figure 3

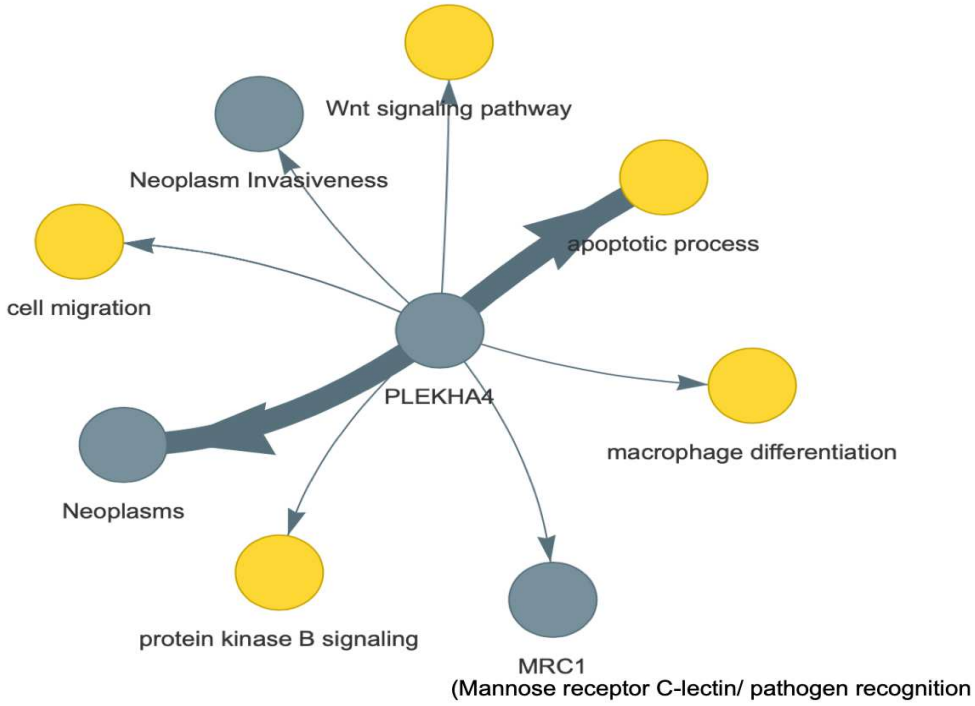
Wnt signaling pathway
Neoplasm Invasiveness
apoptotic process
cell migration
PLEKHA4
macrophage differentiation
Neoplasms
protein kinase B signaling
MRC1
(Mannose receptor C-lectin/ pathogen recognition

Figure 4

A

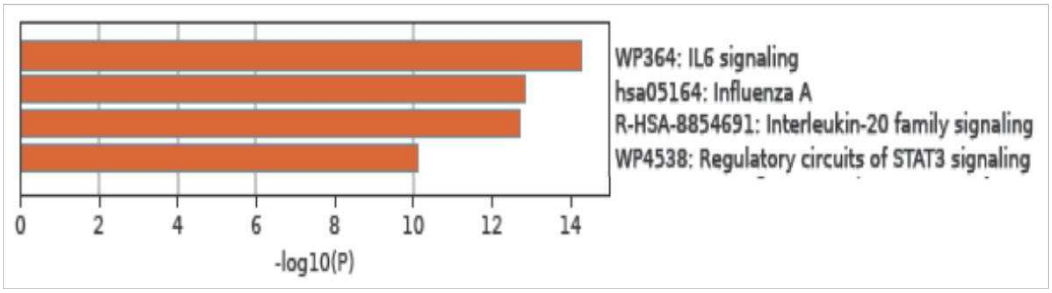
WP364: IL6 signaling
hsa05164: Influenza A
R-HSA-8854691: Interleukin-20 family signaling
WP4538: Regulatory circuits of STAT3 signaling
0
2
4
6
8
10
12
14
-log10(P)

B

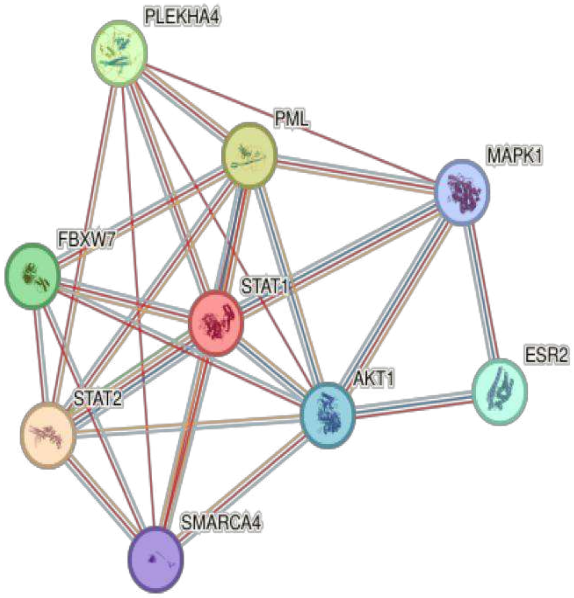
PLEKHA4
PML
MAPK1
FBXW7
STAT1
ESR2
AKT1
STAT2
SMARCA4

Figure 5

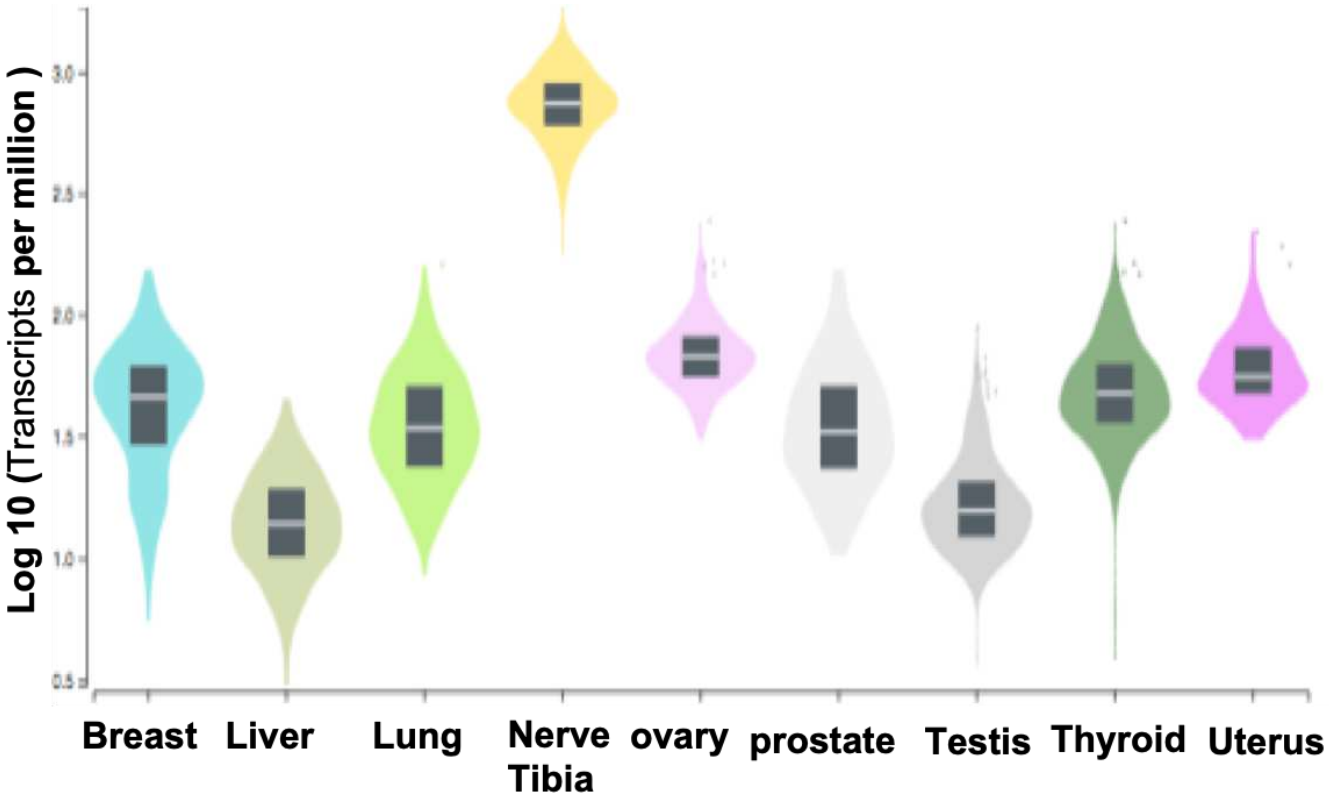
Log 10 (Transcripts per million)
3.0
2.5
2.0
1.5
1.0
0.5
Breast
Liver
Lung
Nerve Tibia
ovary
prostate
Testis
Thyroid
Uterus

Figure 6

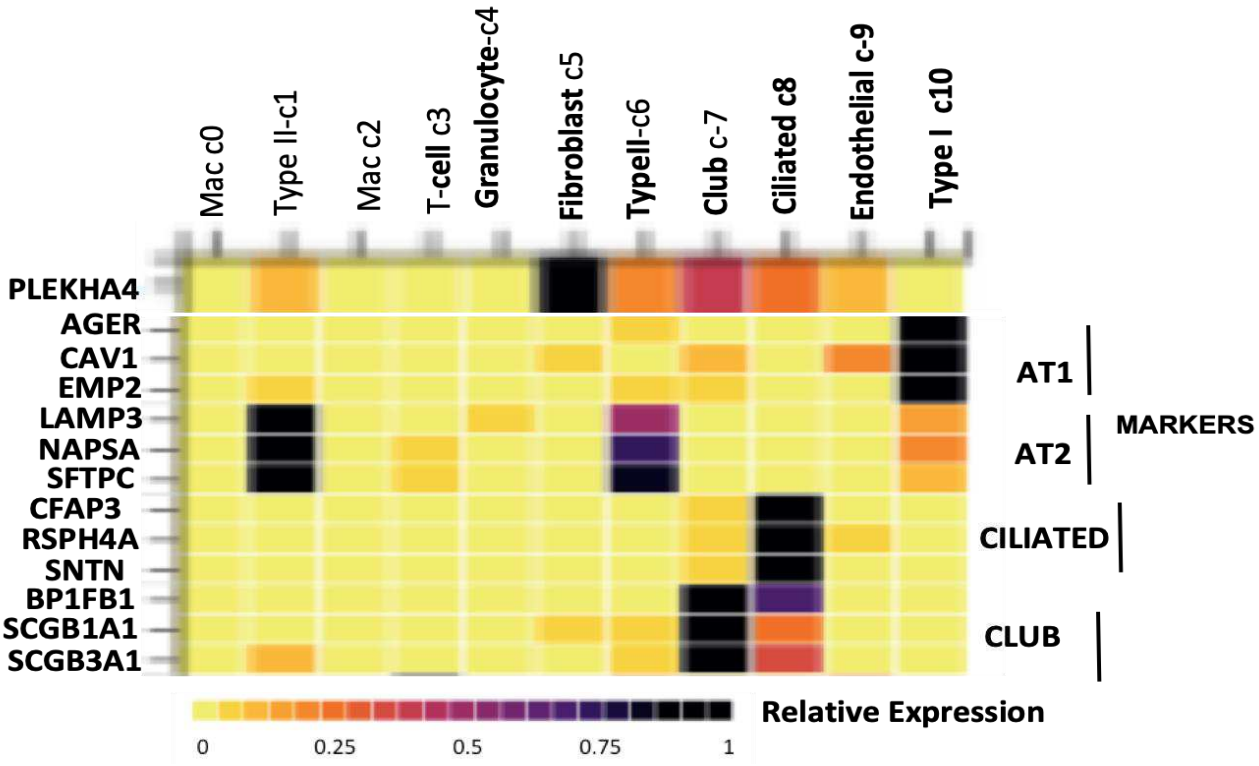
Mac c0
Type II-c1
Mac c2
T-cell c3
Granulocyte-c4
Fibroblast c5
TypeII-c6
Club c-7
Ciliated c8
Endothelial c-9
Type I c10
PLEKHA4
AGER
CAV1
EMP2
LAMP3
NAPSA
SFTPC
CFAP3
RSPH4A
SNTN
BP1FB1
SCGB1A1
SCGB3A1
AT1
AT2
MARKERS
CILIATED
CLUB
Relative Expression
0
0.25
0.5
0.75
1

Figure 7

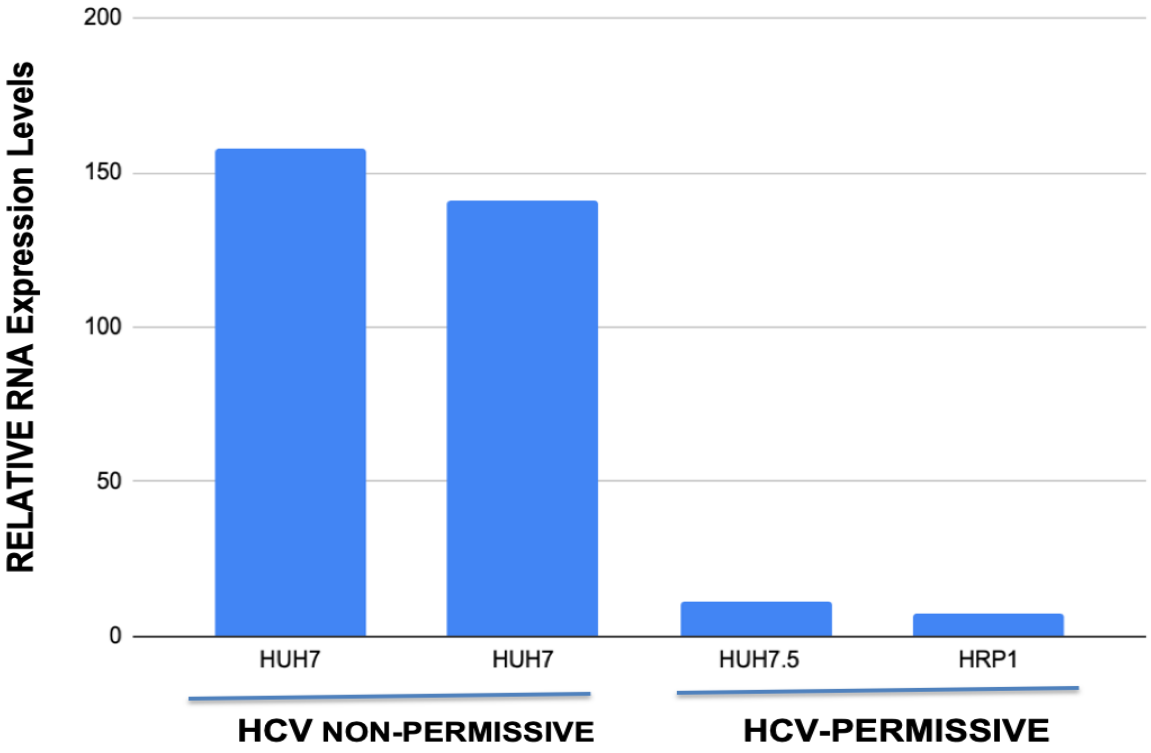
RELATIVE RNA Expression Levels
200
150
100
50
0
HUH7
HUH7
HUH7.5
HRP1
HCV NON-PERMISSIVE
HCV-PERMISSIVE

Figure 8

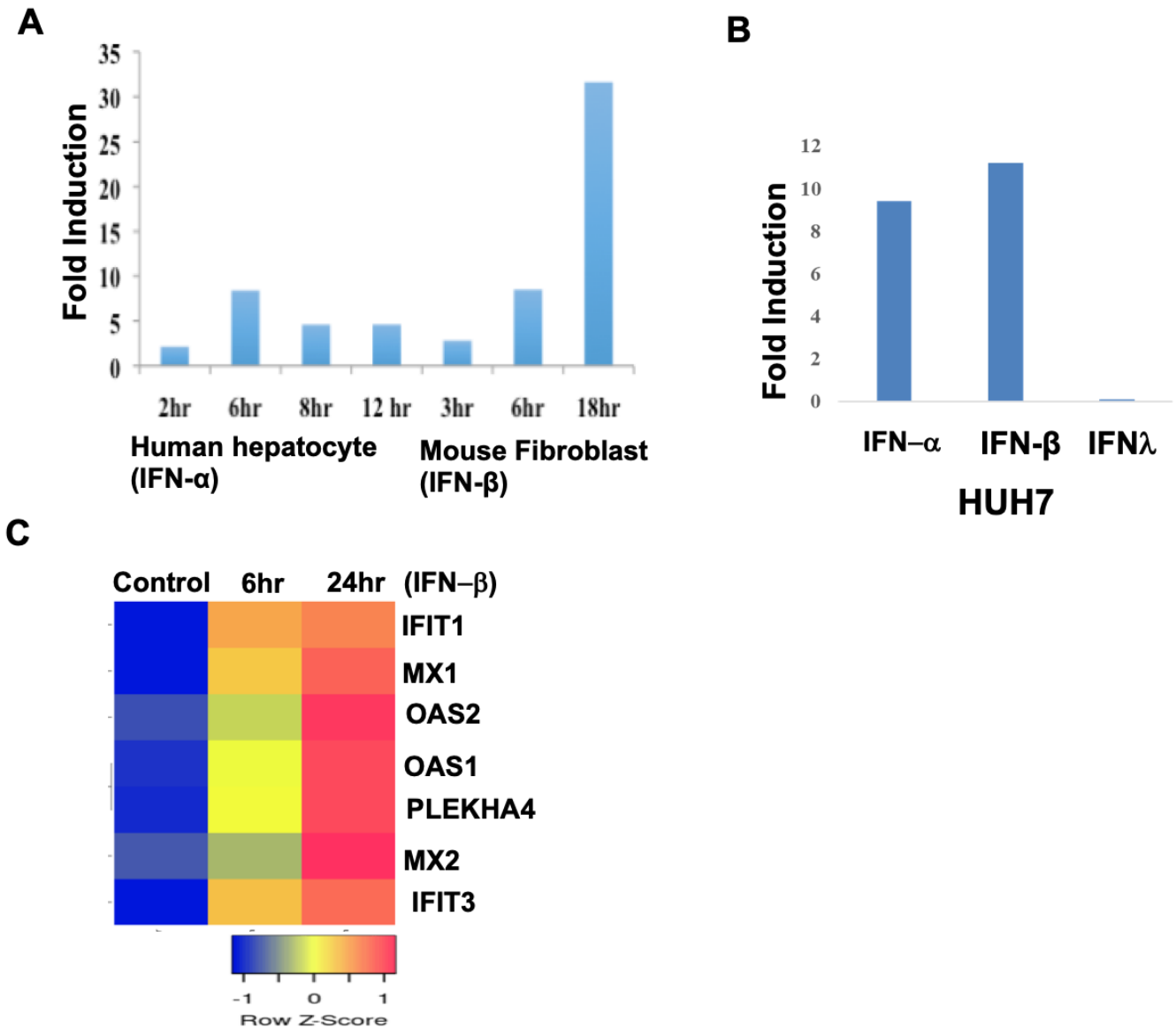
A
Fold Induction
35
30
25
20
15
10
5
0
2hr
6hr
8hr
12 hr
3hr
6hr
18hr
Human hepatocyte
(IFN-α)
Mouse Fibroblast
(IFN-β)
B
Fold Induction
12
10
8
6
4
2
0
IFN–α
IFN-β
IFNλ
HUH7
C
Control
6hr
24hr
(IFN–β)
IFIT1
MX1
OAS2
OAS1
PLEKHA4
MX2
IFIT3
-1
0
1
Row Z-Score

Figure 9

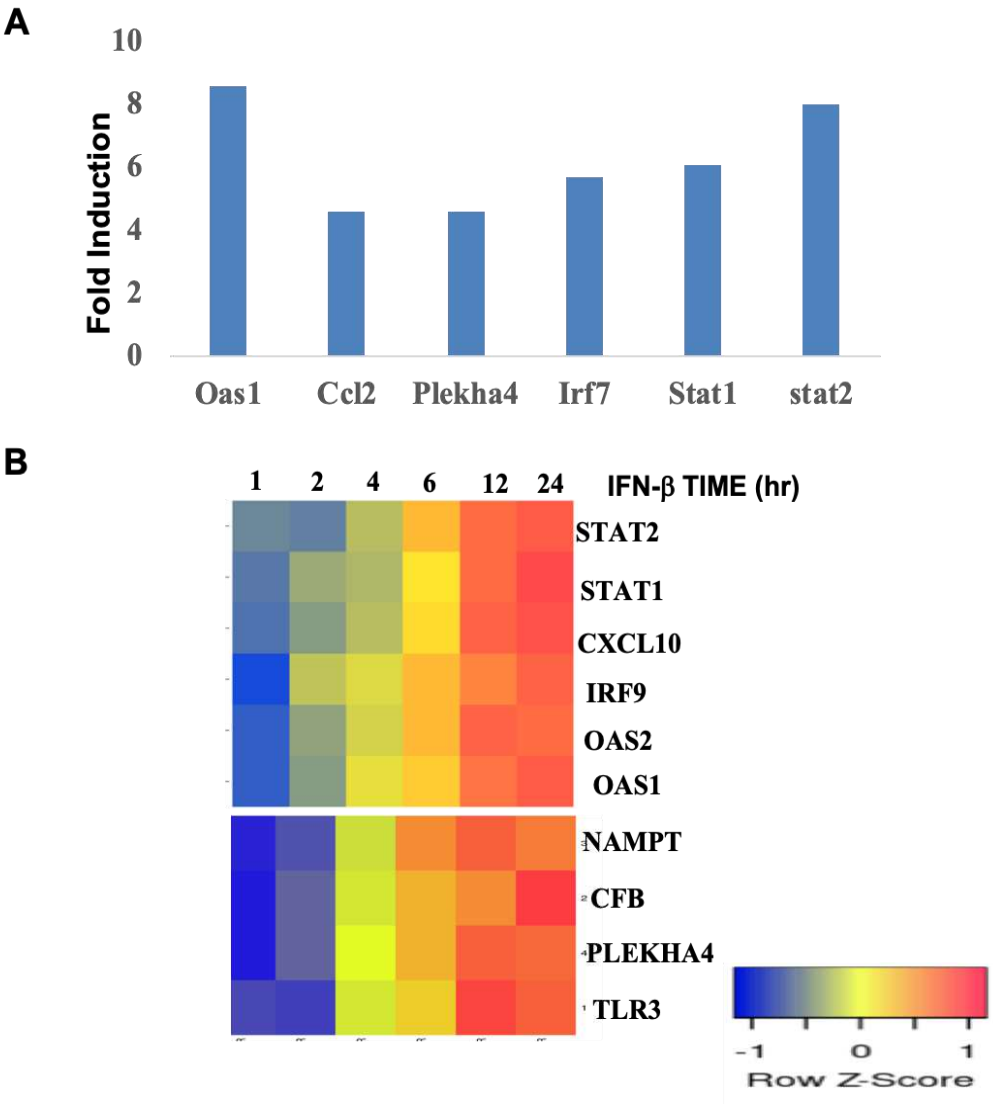
A
Fold Induction
10
8
6
4
2
0
Oas1
Ccl2
Plekha4
Irf7
Stat1
stat2
B
1
2
4
6
12
24
IFN-β TIME (hr)
STAT2
STAT1
CXCL10
IRF9
OAS2
OAS1
NAMPT
CFB
PLEKHA4
TLR3
-1
0
1
Row Z-Score

Figure 10

A

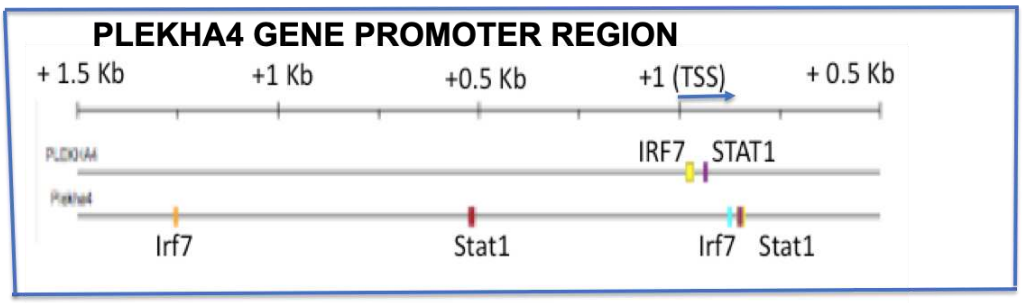

B

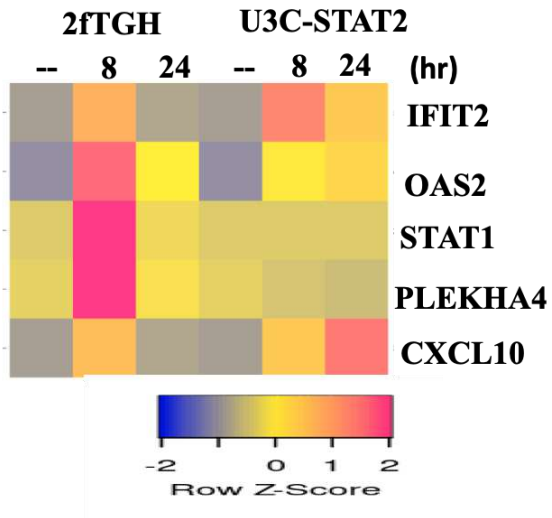

C

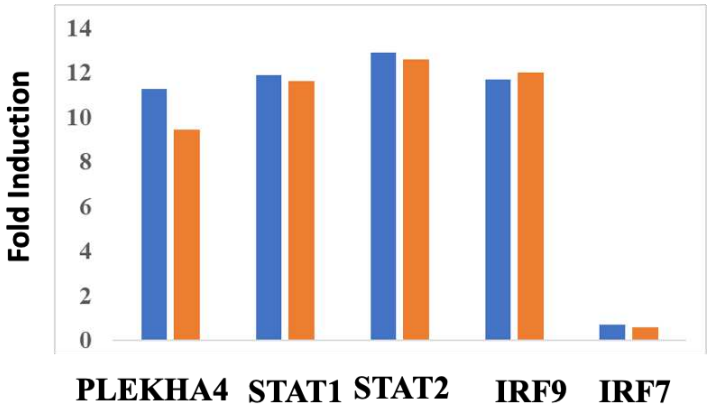

Figure 11

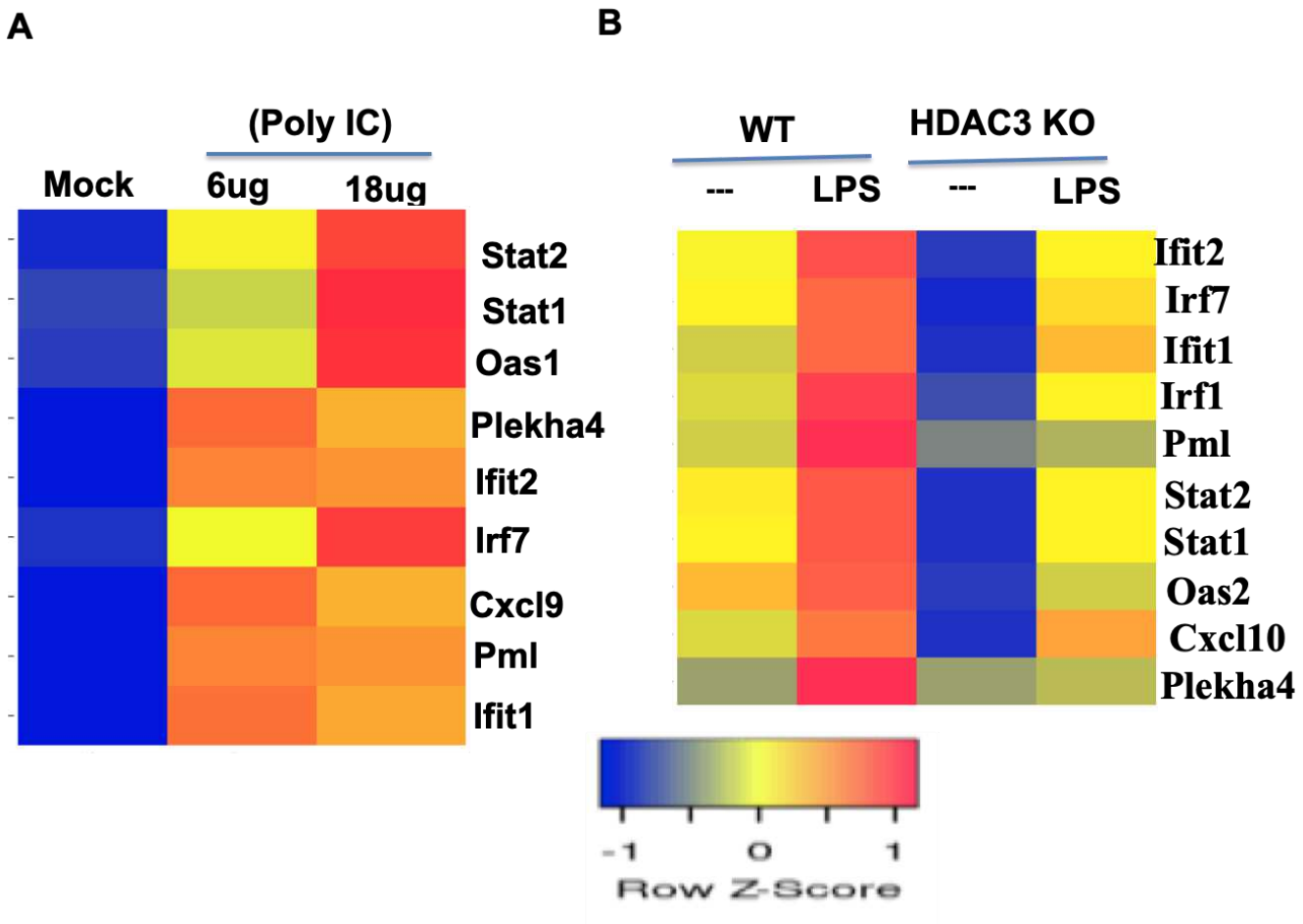
A
(Poly IC)
Mock
6ug
18ug
Stat2
Stat1
Oas1
Plekha4
Ifit2
Irf7
Cxcl9
Pml
Ifit1
B
WT
HDAC3 KO

LPS

LPS
Ifit2
Irf7
Ifit1
Irf1
Pml
Stat2
Stat1
Oas2
Cxcl10
Plekha4
-1
0
1
Row Z-Score

Figure 12

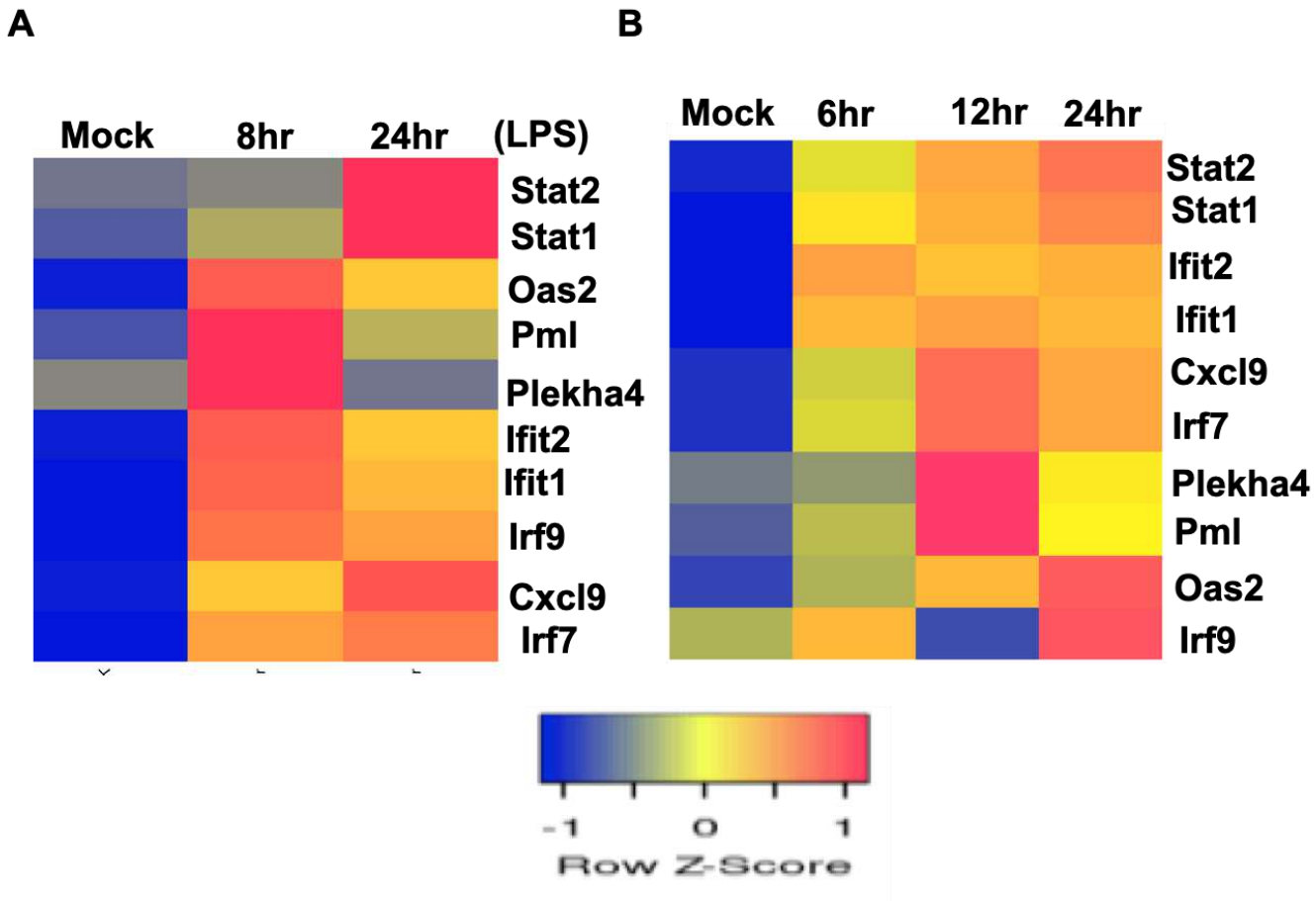
A
Mock
8hr
24hr
(LPS)
Stat2
Stat1
Oas2
Pml
Plekha4
Ifit2
Ifit1
Irf9
Cxcl9
Irf7
B
Mock
6hr
12hr
24hr
Stat2
Stat1
Ifit2
Ifit1
Cxcl9
Irf7
Plekha4
Pml
Oas2
Irf9
-1
0
1
Row Z-Score

Figure 13

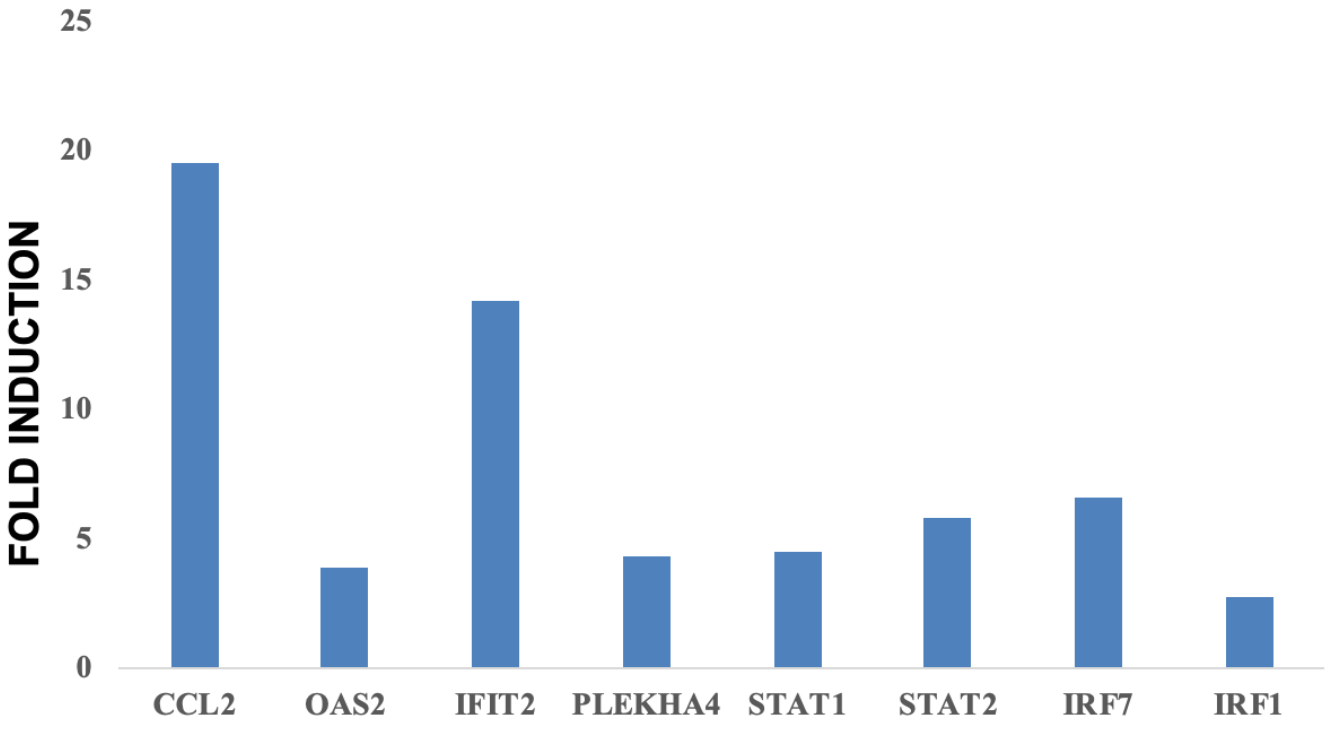
FOLD INDUCTION
25
20
15
10
5
0
CCL2
OAS2
IFIT2
PLEKHA4
STAT1
STAT2
IRF7
IRF1

Figure 14

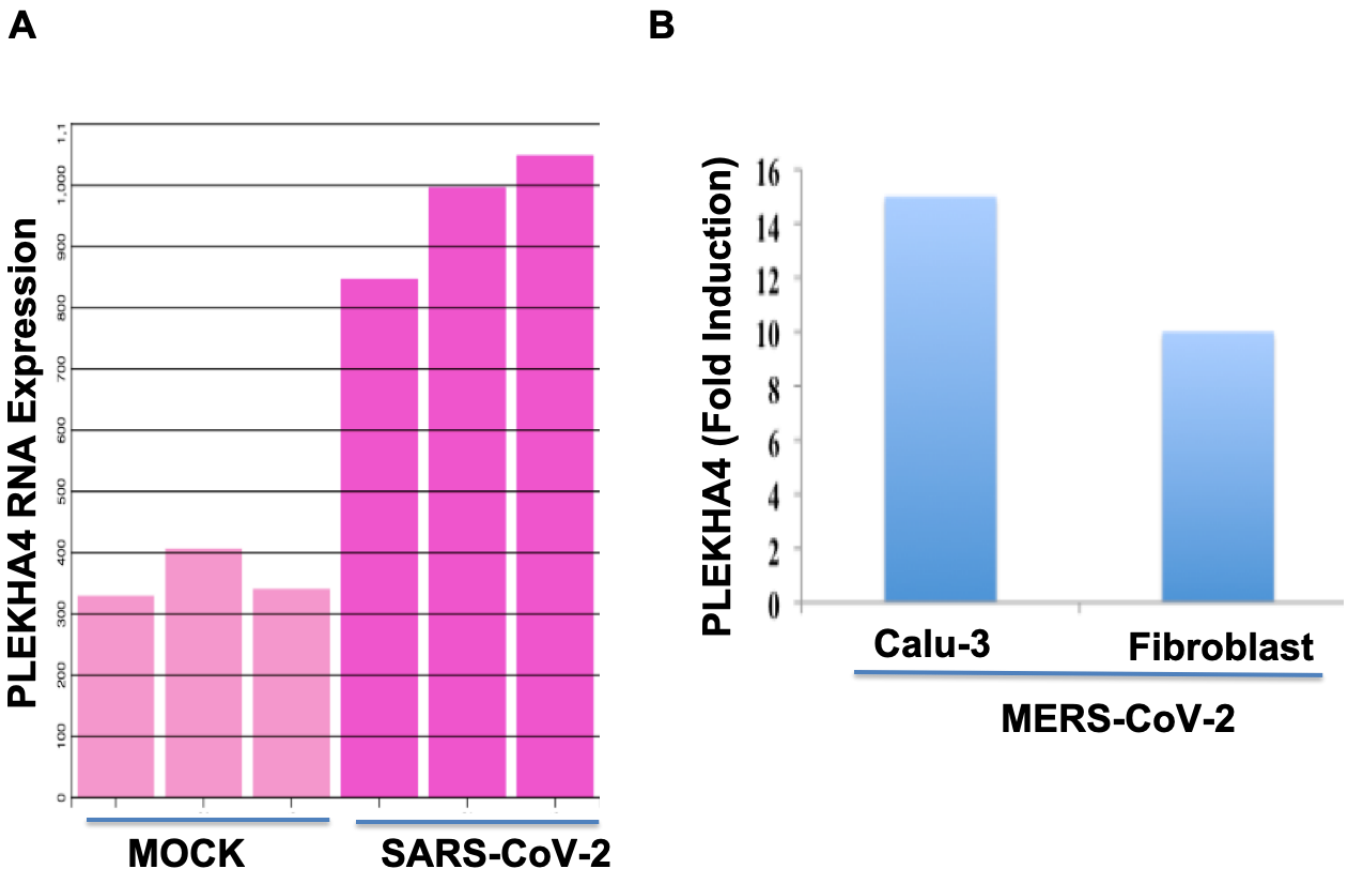
A
PLEKHA4 RNA Expression
0
100
200
300
400
500
600
700
800
900
1,000
1,1
MOCK
SARS-CoV-2
B
PLEKHA4 (Fold Induction)
0
2
4
6
8
10
12
14
16
Calu-3
Fibroblast
MERS-CoV-2

Figure 15

A

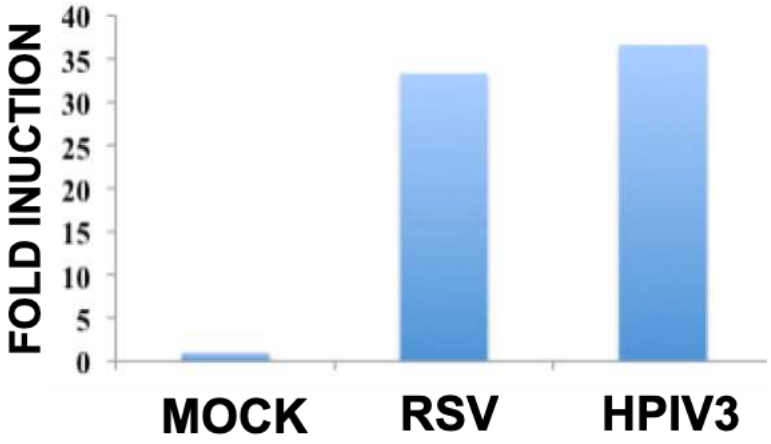
FOLD INUCTION
40
35
30
25
20
15
10
5
0
MOCK
RSV
HPIV3

B

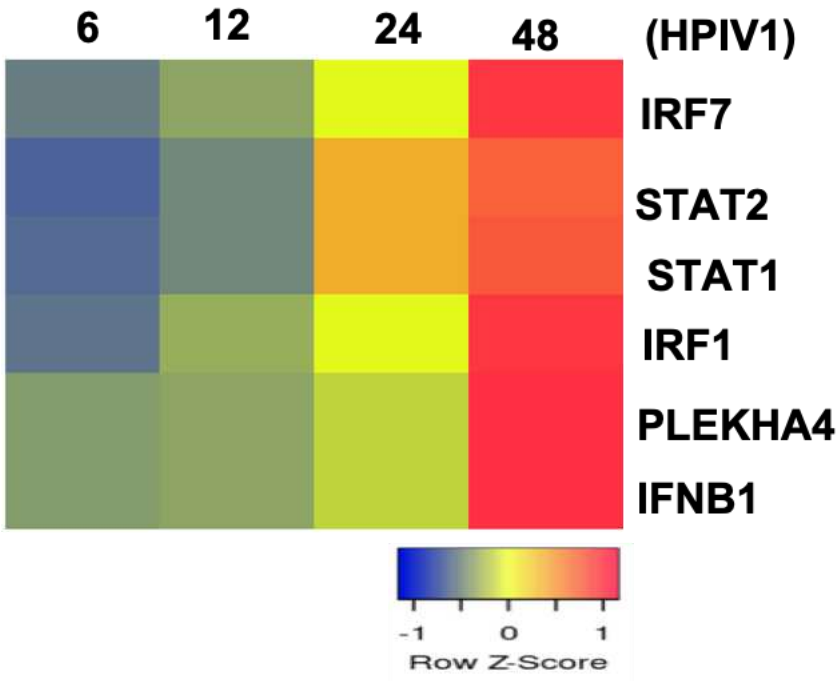
6
12
24
48
(HPIV1)
IRF7
STAT2
STAT1
IRF1
PLEKHA4
IFNB1
-1
0
1
Row Z-Score

Figure 16

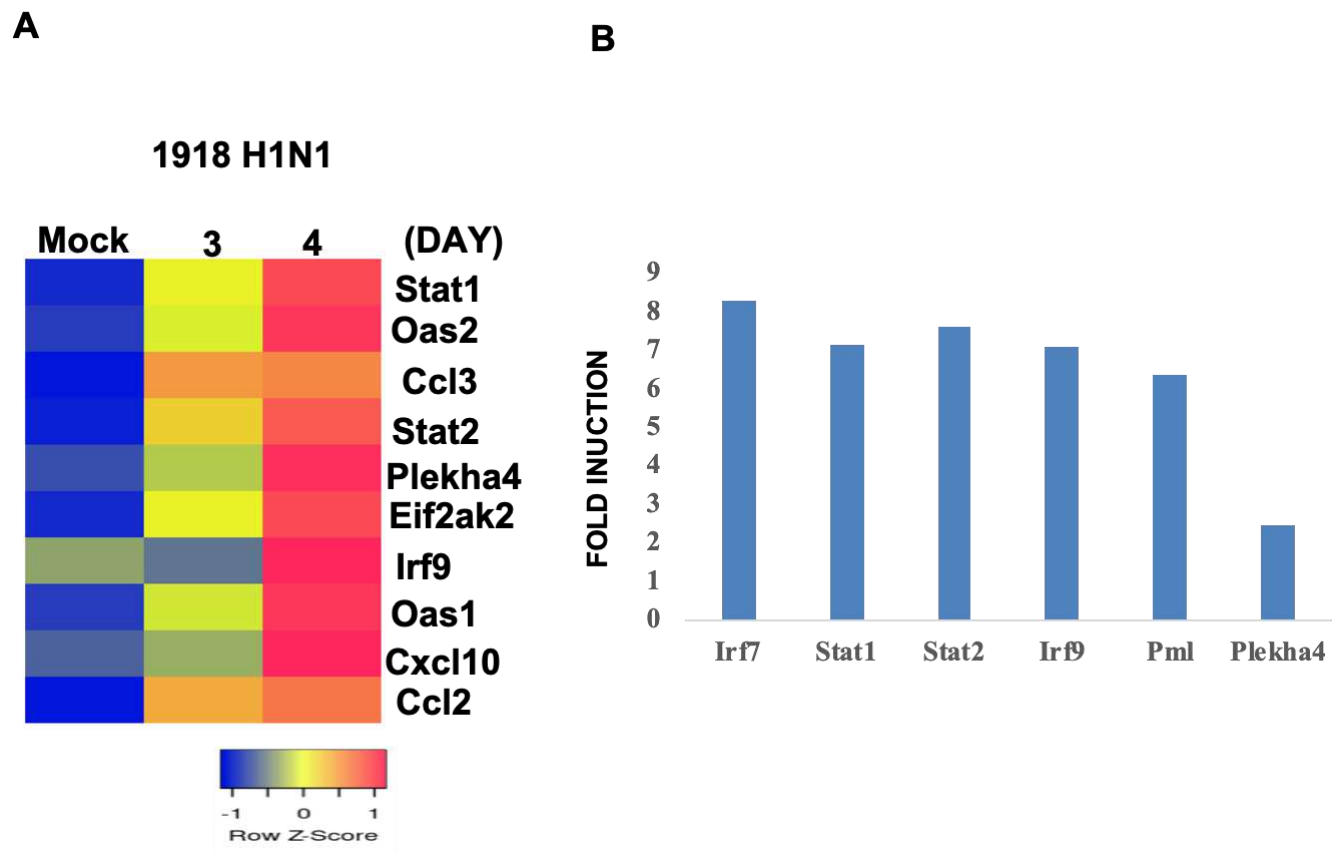
A
1918 H1N1
Mock
3
4
(DAY)
Stat1
Oas2
Ccl3
Stat2
Plekha4
Eif2ak2
Irf9
Oas1
Cxcl10
Ccl2
-1
0
1
Row Z-Score
B
FOLD INUCTION
9
8
7
6
5
4
3
2
1
0
Irf7
Stat1
Stat2
Irf9
Pml
Plekha4

Supplementary Figure 1

